Institute of Paper Science and Technology

IMPULSE DRYING OF LINERBOARD: EVALUATION OF A PROTOTYPE CERAMIC COATED PRESS ROLL

Project 3470

REPORT THREE

to

MEMBER COMPANIES OF

THE INSTITUTE OF PAPER SCIENCE AND TECHNOLOGY

June 1991

Atlanta, Georgia

INSTITUTE OF PAPER SCIENCE AND TECHNOLOGY

Atlanta, Georgia

IMPULSE DRYING OF LINERBOARD:EVALUATION OF A PROTOTYPE CERAMIC COATED PRESS ROLL

Project 3470

Report 3

By

David I. Orloff

A Yearly Progress report to Institute Member Companies

June, 1991

TABLE OF CONTENTS

BASIC UNITS AND CONVERSIONS

Mass	Kilograms (kg) = 2.20462 pound mass (lb_m) Ton = 2000 lb_m.
Length	Meters (m) = 3.2808 feet (ft).
Time	Second (s) = 1000 milliseconds (ms).
Volume	Cubic meters (m^3) = 10^6 milliliters (mL).
Force	Newton (N) = 0.22481 pound force (lb_f).
Pressure	Pascal (Pa) = 0.000145 pounds per square inch(psi). MegaPascal (MPa) = 1 x 10^{+6} Pascal.
Temperature	Degree Celsius (°C) Degree Fahrenheit (°F) = °C x (9/5) + 32.
Energy	Joule (J) = 9.486 x 10^{-4} British Thermal Units (Btu). Quad = 1 x 10^{+15} Btu.
Power	Watt (W) = 1 J/s Watt (W) = 9.486 x 10^{-4} (Btu/s).

SYMBOLS AND ABBREVIATIONS

α	Thermal diffusivity, m^2/s.
C'	Constant defined in equation 1.
C_p	Specific heat, $W\cdot s/g\cdot{}^\circ K$.
CSF	Canadian standard freeness, (mL). TAPPI Method T227 OM-85.
CVSEM	Coefficient of variation of the specific elastic modulus, (%).
Burst Index	Burst strength index, $kPa\cdot m^2/g$. Tappi Method T807.
K	Ratio of the thermal conductivity to the square root of the thermal diffusivity, $W\cdot s^{1/2}/m^2\cdot{}^\circ K$.
KAPPA No.	Kappa Number. Tappi Method T236 CM-85.
λ	Thermal conductivity, $W/m\cdot{}^\circ K$.
ρ	Density, g/m^3.
SEM	Specific elastic modulus, MN·m/kg.
STFI Index	Compressive strength measured by STFI method, (N·m/g). Tappi Method T826 pm.86.
V	Pore volume fraction.

SUMMARY

The pulp and paper industry is one of the largest industrial consumers of energy in the United States. Based on thirty million BTU's per ton of paper produced and annual production of 76 million tons, a total of 2.3 Quads are consumed by the industry annually. Drying is the largest single energy use in the papermaking process and accounts for about one quarter of the energy used.

Impulse drying is an innovative process for drying paper that holds great promise for reducing the energy consumed during the manufacture of paper and similar web products. Impulse drying occurs when a wet paper web passes through a press nip in which one of the rolls is heated to a high temperature. A steam layer adjacent to the heated surface grows and displaces water from the sheet in a very efficient manner. The energy required for water removal is very much less than that required for conventional evaporative drying. Hence, it has been projected that wide commercialization of impulse drying would result in at least a 10% industry-wide energy saving.

Early attempts to commercialize the process were frustrated by the occurrence of sheet delamination. Research supported by the Office of Industrial Programs of the Department of Energy has focused on resolving this major technical obstacle to commercialization.

Previous research addressed the mechanisms responsible for sheet delamination. It was postulated that, as the nip depressurizes, superheated water remaining in the sheet flashes to vapor and escapes through the sheet surface. When excessive amounts of energy are transferred to the sheet, drag forces resulting from the escaping vapor can be high enough to overcome the cohesive forces holding the sheet together and the sheet delaminates.

To eliminate sheet delamination, the Institute has taken the approach of controlling energy transfer to the sheet. Low "thermal mass" ceramic press roll coatings were developed to reduce heat transfer to the sheet, while maintaining high heat flux during early stages of the process. In so doing, most of the transferred energy is used to form steam that displaces liquid water, rather than in excessively heating the sheet.

This report covers work completed between July, 1990 and June, 1991. During this period, a prototype ceramic coating was developed and its impulse drying performance was compared to that of steel surfaces. It was observed that ceramic platens can be operated at higher temperatures and pressures resulting in improved water removal and physical properties without inducing sheet delamination. Heat flux measurement techniques were developed to provide a mechanistic explanation for the superior performance of the prototype. The work confirmed that the prototype ceramic coating is more energy efficient than the steel surface. In contrast to the case of a steel impulse drying surface, energy transfer from the prototype surface was found to be pressure independent. This strongly suggests that by reducing the thermal mass of the impulse drying surface, energy transfer becomes independent of the state of the paper being impulse dried.

Encouraged by these laboratory-scale simulations, the pilot impulse dryer was retrofitted with a prototype ceramic coated press roll and was used to evaluate its performance in impulse drying single-ply linerboard. Pilot-scale experiments were conducted over a range of ingoing solids and nip residence times at a single refining level consistent with industrial practice. In terms of water removal, energy efficiency and property development, the results of the pilot evaluation were even more impressive than the laboratory-scale work. For maximum benefit, ingoing solids should be greater than 40% and nip widths capable of minimum nip residence times of 40 ms are recommended.

These results encourage us to propose a commercialization project that will facilitate the introduction of impulse drying technology in the United States.

OVERVIEW AND OBJECTIVES

The impulse drying process under development at IPST employs a heated roll press to activate a more efficient water removal mechanism. During the process, wet paper is brought into contact with a hot press roll, typically heated to between 200°C and 400°C, while pressures between 3 MPa and 6 MPa are maintained in the sheet for times between 20 to 40 milliseconds.

The water removal mechanism is different from that involved in conventional wet pressing and evaporative drying processes. Previous research (1-3) has shown that, during impulse drying, high pressure steam is generated rapidly at or near the interface between the sheet and the heated roll surface. As moisture is converted to steam by heat transferred from the hot roll, the steam layer grows and displaces liquid water from the sheet into a water receiver, typically a press felt. As most of the water is removed in the liquid phase, as opposed to conventional drying where all of the water is evaporated, there is a large energy saving.

As the impulse drying process is terminated before the sheet is completely dried, flash evaporation of residual water within the sheet results in a distinctive density profile through the sheet, characterized by dense surface layers and a bulky midlayer. For some grades and conditions, this translates into improved physical properties. For other grades, flash evaporation can cause delamination of the sheet.

In early simulations, Arenander and Wahren (4) and Burton (5,6) reported delamination during intense impulse drying. Thereafter, delamination was viewed as a phenomenon that would be encountered only under extreme conditions easily avoided in commercial practice.

However, during a joint feasibility study by Beloit Corporation, Weyerhaeuser Company and IPST, delamination emerged as a major problem. As reported by Crouse, Woo and Sprague (7), various degrees of delamination were experienced with linerboard impulse dried at press roll surface temperatures above 150°C. When delamination was avoided by operating below this limit, water removal efficiencies were not significantly different from those obtained by conventional pressing. Hence, it was concluded that to realize the potential of impulse drying, it would be necessary to alleviate delamination.

Based on the hypothesis that delamination occurs when excess energy is transferred to the sheet, Orloff (8) and Santkuyl (9) investigated various alternate platen materials that were expected to alter the heat flux to the sheet during the impulse drying event. These included two solid platens, one of steel and one of aluminum, as well as two porous platens made from sintered stainless steel, at two different porosities. Although the heat flux from the aluminum platen was expected to be substantially higher than that for the steel platen, the effect on delamination was found to be negligible. The porous platens, were expected to result in a lower heat flux and to provide venting of steam generated at the platen /sheet interface. While experiments with the porous platens showed no evidence of delamination, water removal was substantially reduced. Analysis of the mass of water transferred to the felt compared to the mass of water lost from the sheet confirmed that significant steam venting occurred. Venting and the associated reduction in steam pressure are consistent with the observation of reduced water removal as the impulse drying mechanism is suppressed. An additional consequence of venting is a reduction in energy efficiency.

In a recent patent application, Orloff (10) demonstrated that non-porous low-thermal mass-surfaces made from machinable ceramics could be used to extend the range of impulse drying operating conditions while avoiding sheet delamination. Preliminary experiments by Orloff (11) showed that these materials operate by reducing heat transfer to the sheet during nip depressurization. Such a reduction results in lower average sheet temperatures and less delamination inducing flash vaporization.

More practical roll coating materials have been investigated by Orloff (12). Using plasma-sprayed ceramic coatings sealed with high-temperature polymers, 205 gsm linerboard was impulse dried from 30% solids for dwell times of 20 ms. The experiments showed that plasma-sprayed ceramic coatings have the potential for extending the maximum roll surface operating temperature and achieving impressive water removal without inducing sheet delamination.

The work performed during the current period included (1) developing an understanding of the mechanism of operation of ceramic surfaces for delamination control, (2) demonstrating the technology on the pilot scale for single-ply linerboard and (3) exploring various concepts to further improve the performance of impulse drying surfaces.

PROGRESS IN IMPULSE DRYING RESEARCH

PLANS FOR THE PERIOD

The overall objective of this project was to overcome the problem of sheet delamination for heavyweight grades of paper. To support that objective, the following tasks were accomplished:

1. Using the electrohydraulic press, a set of baseline master pressing curves were developed to show the influence of operating conditions, such as ingoing sheet moisture, preheat temperature and impulse, on single felted wet pressing of 205 gsm single-ply linerboard. The results of this task are reported in the Appendix.

2. Using the electrohydraulic press, a set of master drying curves was developed to show the influence of operating conditions, such as impulse, ingoing sheet moisture gradients and ingoing platen surface temperature, on impulse drying of 205 gsm single-ply linerboard using both steel and a prototype ceramic coated platen. Maximum moisture ratio change, defined by the onset of sheet delamination, was also determined. In addition, heat flux measurements during the impulse drying process were used to help understand the mechanism of operation of the prototype ceramic surfaces and to document their enhanced energy efficiency.

3. An existing steel pilot roll was coated with the prototype ceramic coating for evaluation on the infrared heated nip of the pilot dryer. Master drying curves and maximum moisture ratio change were determined by impulse drying 205 gsm single-ply linerboard over a range of nip residence times and ingoing dryness. The laboratory scale impulse drying simulator was then used to determine energy utilization at these conditions.

IMPULSE DRYING PERFORMANCE OF THE PROTOTYPE PLATEN

Experimental Methods

Figure 1 shows a schematic of the electrohydraulic press used to simulate single felted pressing and impulse drying. In the experiments of this study, handsheets were pre-steamed to 85°C prior to pressing or impulse drying.

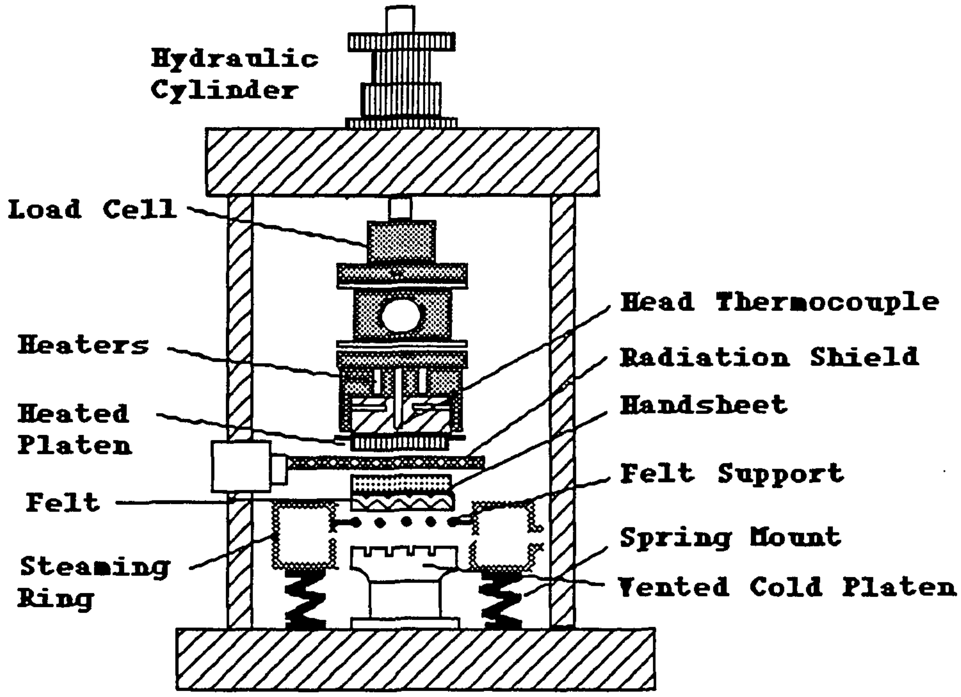

Figure 1: Schematic of the electrohydraulic press.

Figure 1 shows the pre-steaming configuration. Pre-weighed handsheets were placed on pre-weighed felts, which were then placed onto a wire felt support attached to a preheated steaming ring. Depending on the experiment, a radiation shield could be automatically positioned between the heated platen and the sheet to reduce dry-out of the top surface of the sheet. Steam exiting the ring flowed upward through the felt and the handsheet. By controlling steam pressure to 105 KPa and adjusting the steaming time and wait time before pressing or impulse drying, the initial temperature in the handsheet could be controlled.

The steam pre-heat can uniformly raise the temperature of the sheet. Figure 2 shows internal handsheet temperatures during steaming and during the wait period (when steam flow was discontinued) for a 205 gsm handsheet composed of four 50 gsm layers steamed without the radiation shield under an 80°C steel platen.

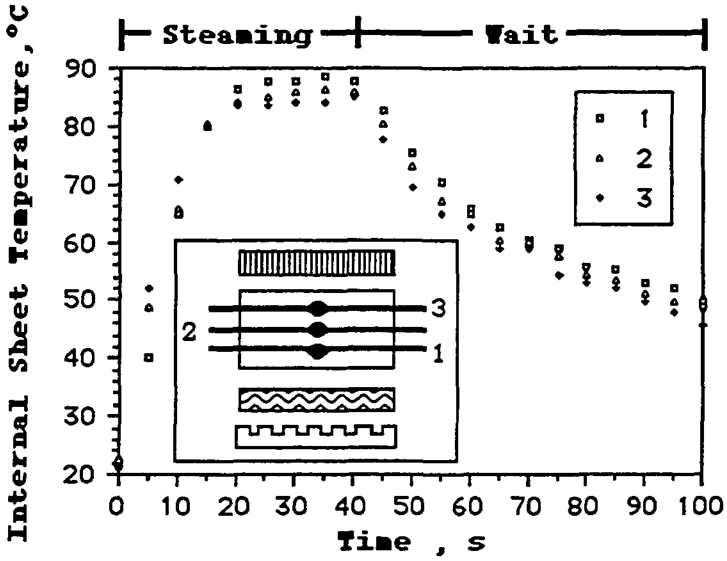

Figure 2: Internal sheet temperature of 205gsm linerboard as a function of time during steaming and wait period. Steel platen temperature=85°C without radiation shield.

The temperature gradient through the center of the sheet was less than 3°C after 40 seconds of steaming and less than 4°C after a wait period of 60 seconds. When the platen temperature was raised to 315°C, as shown on Figure 3, the temperature gradient through the center of the sheet was less than 4°C after 40 seconds steaming and less than 2°C after a wait period of 60 seconds.

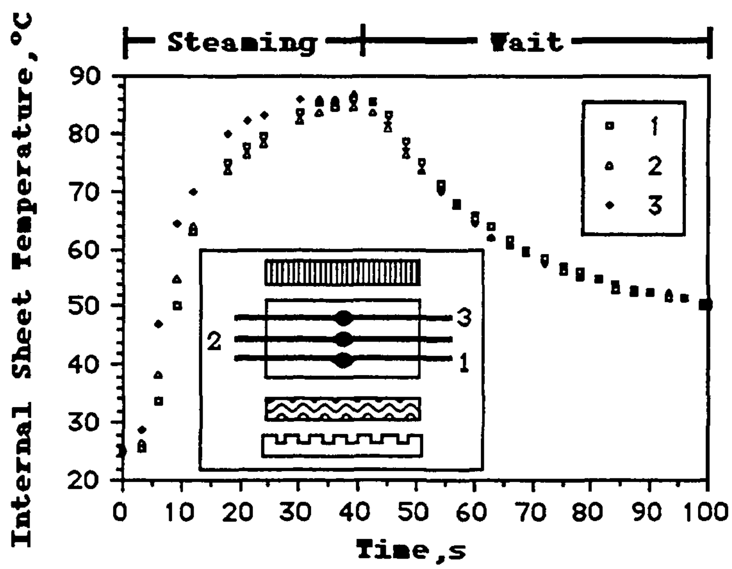

Figure 3: Internal sheet temperature of 205gsm linerboard as a function of time during steaming and wait period. Steel platen temperature=315°C without radiation shield.

In single felted pressing simulations, the platen surface was maintained at the temperature of the preheated (steamed) handsheet so that there was little if any loss of moisture due to surface evaporation. However, impulse drying simulations required a range of initial platen surface temperatures from a low value equal to the ingoing handsheet temperature to a high of as much as 500°C. At high platen surface temperatures, thermal radiation during steaming can result in a substantial moisture loss. To maintain constant initial handsheet moisture prior to impulse drying, the moisture of handsheets prior to steam preheating was adjusted so that, once steamed, their average moisture was 30% solids. Figure 4 and 5 show the change in handsheet weight due to steam preheating for 40 seconds while the platen surface temperature was held constant over a range of temperatures. For these calibration experiments, performed with and without the radiation shield, handsheet ingoing solids were 30% solids while ingoing felt moisture was 16%. Experiments starting at an ingoing solids of 25% showed identical results. Therefore, over a range of ingoing dryness from 25% to 30%, weight changes due to steaming with and without the radiation shield could be predicted from Figures 4 and 5 for both steel and prototype ceramic coated platens.

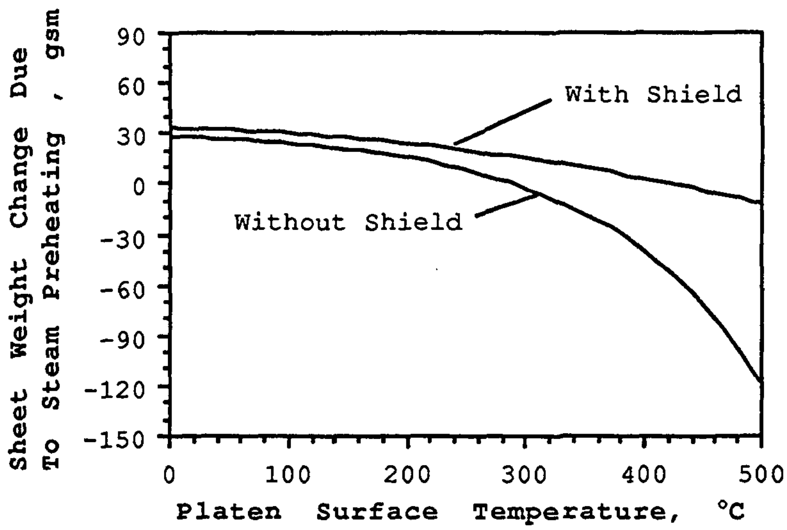

Figure 4: Sheet weight change due to steaming a 205 gsm linerboard sheet for 40 seconds as a function of platen surface temperature for the steel platen with and without the radiation shield.

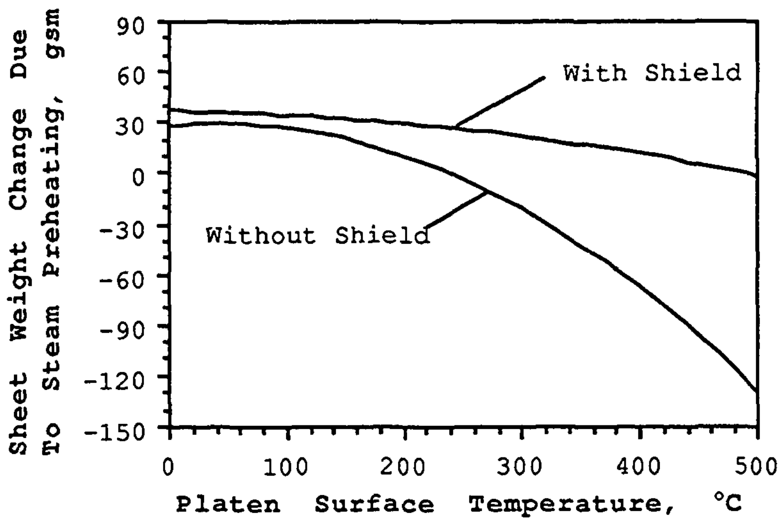

Figure 5:* *Sheet weight change due to steaming a 205 gsm linerboard sheet for 40 seconds as a function of platen surface temperature for the prototype ceramic coated platen with and without the radiation shield.

Use of the radiation shield during sheet preheating significantly reduces sheet evaporative losses.

The average dryness of a sheet prior to impulse drying can be controlled by adjusting the pre-steamed sheet dryness to account for evaporation. However, such an adjustment does not correct moisture gradients induced into the sheet. To show how the radiation shield prevents excessive moisture gradients, layered sheets were used to estimate these gradients. For this purpose, 205 gsm linerboard sheets were made by layering three 51 gsm sheets and two 26 gsm sheets. The moisture in each layer was adjusted to 30% solids just prior to layering. The resulting layered sheet was subjected to steam preheating with and without the radiation shield. The experiments were performed with the prototype ceramic coated platen at two platen surface temperatures.

After steaming, each layer was weighed to determine the moisture profile through the sheet. As the sheet weight change of layered sheets was similar to that of unlayered sheets, layering was expected to have little effect on moisture gradient measurements.

The moisture profile through the sheet was expected to be a function of the initial moisture profile, the amount of steam injected into the sheet, radiant heat transfer to the sheet and diffusion of water within the sheet. In the experiments, the steam flow rate was held constant while the platen temperature was set at 300°C and 480°C with and without the radiation shield.

The differences in moisture profile are due to different amounts of radiant heat transfer to the sheet. The moisture profiles, presented in Figures 6 through 9, represent averages of at least five observations per condition. The moisture of a given layer is reported as percent solids and is ascribed to the center of the layer.

Figures 6 through 9 show that, at high initial platen surface temperatures, the top surface of the sheet can dry out if not protected by the radiation shield.

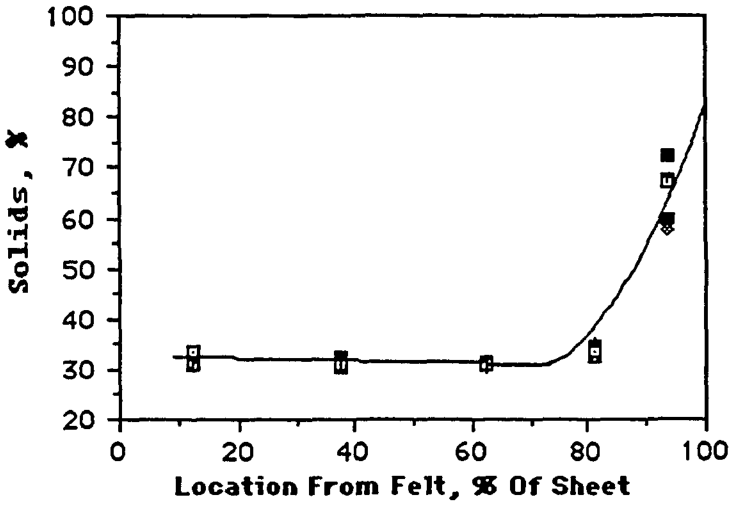

Figure 6: Moisture gradient in sheets after preheating to 85°C under the prototype ceramic coated platen at a platen temperature of 296°C without the radiation shield.

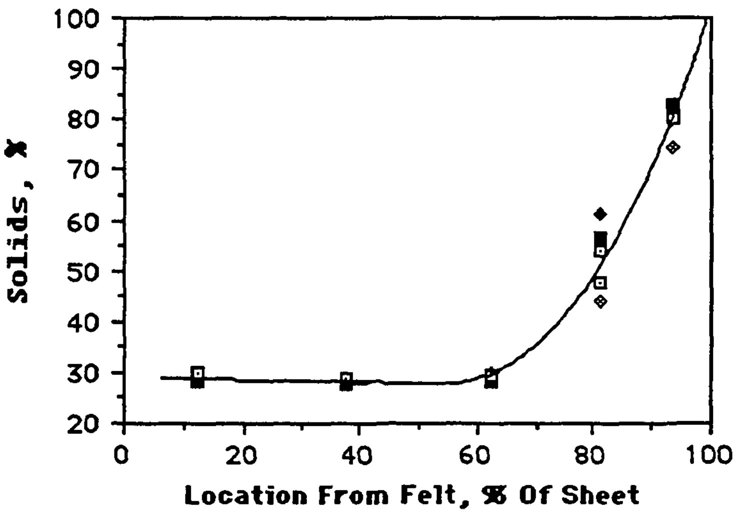

Figure 7: Moisture gradient in sheets after preheating to 85°C under the prototype ceramic coated platen at a platen temperature of 482°C without the radiation shield.

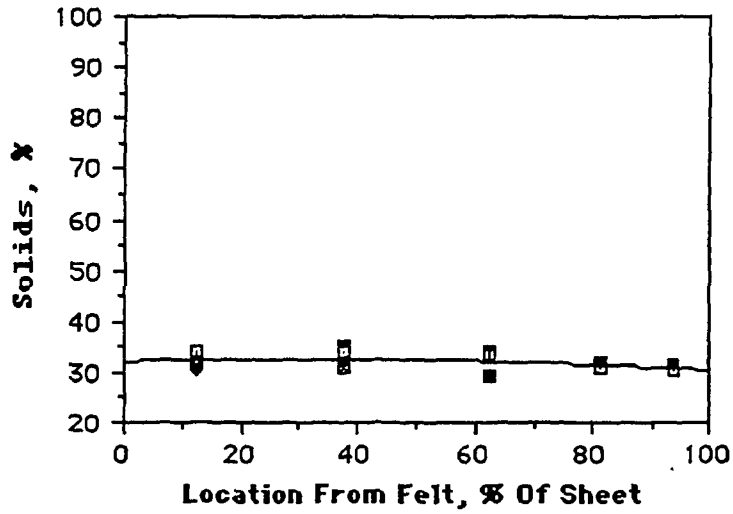

Figure 8: Moisture gradient in sheets after preheating to 85°C under the prototype ceramic coated platen at a platen temperature of 296°C with the radiation shield.

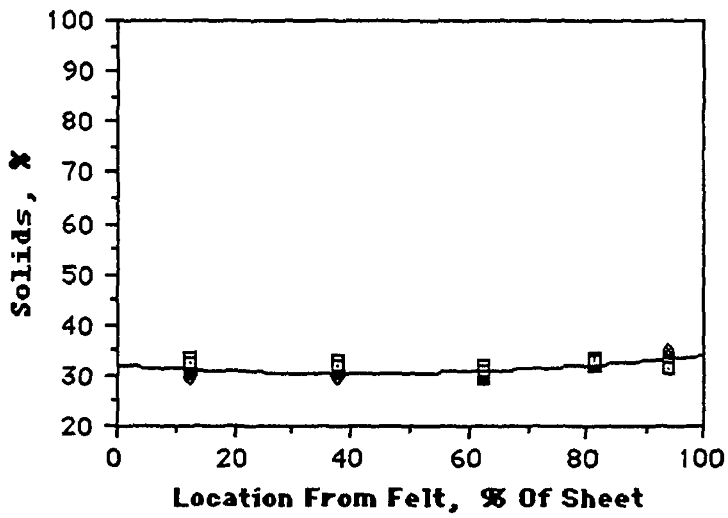

Figure 9: Moisture gradient in sheets after preheating to 85°C under the prototype ceramic coated platen at a platen temperature of 469°C with the radiation shield.

To simulate impulse drying, the heater set-point temperature was adjusted to obtain the desired initial platen surface temperature as measured with a surface thermocouple. Based on the desired platen temperature, handsheets with proper ingoing solids were selected such that they would be at 30.0±0.5% solids after steaming. The basis weight of the handsheets was maintained at 205±10 gsm. Handsheets were positioned such that their wire side was in contact with the felt as shown in Figure 1. Felts made from Nomex fibers, at an ingoing moisture of 16%, were used. A wave generator was used to control the impulse. At the short dwell times of 20 ms, equipment limitations resulted in compression and decompression rates which increased when the peak pressure was increased. Figure 10 shows typical pressure vs. time curves which were reproducible to a precision of ±0.2 MPa peak pressure.

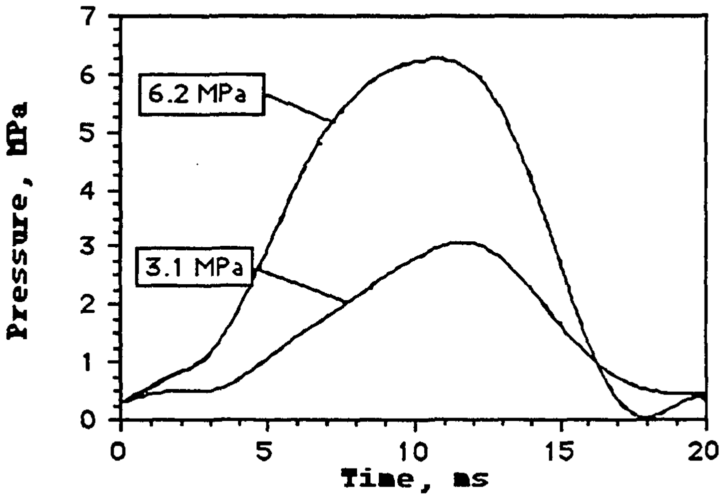

Figure 10: Pressure as a function of time for various peak pressures. Dwell time=20ms.

Throughout the course of the research program, delamination was assessed by visual observation directly after impulse drying and before finish and oven drying. Visible delamination may be classified as either major or minor. Minor delamination consisted of small blisters on the edges of the sheet or pinpoint size blisters on the heated surface of the sample. Major delamination consisted of discrete blisters having a diameter greater than 3 mm.

It was recognized that a quantitative measure for delamination was a necessity. With this in mind, samples were also evaluated using an out-of-plane ultrasonic test method (12,13). The method had the advantage of being non-destructive, sensitive to delamination and predictive of standard destructive tests.

Samples which were impulse dried and finish dried to 95% solids were tested ultrasonically. In the test, the speed of sound through paper was measured between 3/8" diameter soft rubber platens. Using the measured sonic velocity, localized specific elastic modulus (SEM) was determined. By making 12 measurements at various locations on each sample, a coefficient of variation of the specific elastic modulus (CVSEM) was determined.

Blisters on the edges of sheets were typically missed during ultrasonic testing. In addition, very small surface blisters tend to heal during finish drying. Hence, minor delaminations were not generally detected by the ultrasonic test method.

Major delaminations were distinguishable from non-delaminated samples based on the CVSEM. Figure 11 shows the cumulative probability of non-delaminated and major delaminated samples as a function of measured

CVSEM. A critical CVSEM of 10% was chosen as a delamination criterion since 80% of samples showing no visible delamination have CVSEM below 10%, while 75% of samples showing major visible delamination were above a CVSEM of 10%. Hence, a CVSEM equal to or greater than 10% indicates sheet delamination.

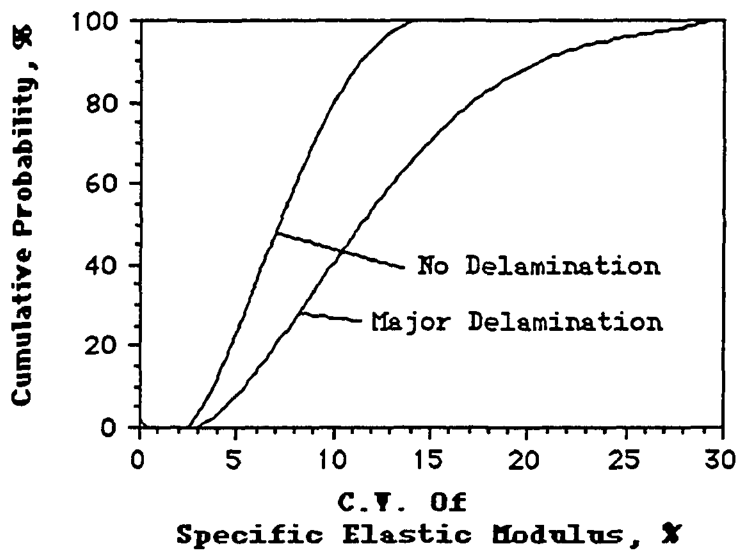

Figure 11: Cumulative probability of finding non-delaminated and major delaminated samples with coefficients of variation of specific elastic modulus less than the given amount.

An objective of the current work was the measurement of heat flux during impulse drying. Both steel- and ceramic-coated platens were to be evaluated in terms of water removal, delamination suppression and energy utilization. Steel platens had previously been instrumented with eroding type probe thermocouples to record surface temperature during impulse drying. These measurements, along with the thermal properties of the steel platen, can be used to calculate instantaneous heat flux from the platen to the sheet of paper being impulse dried. The design of the eroding thermocouples is shown on Figure 12. To function properly, an insert made from the platen material must be used in fabrication. For ceramic-coated platens, the eroding design was impractical, and a ribbon type thermocouple, also shown on Figure 12, was used. In these experiments, the iron constantan ribbon thermocouple bead had a thickness of 0.064 mm and a bead surface area of 3 mm^2. In future work, the influence of thermocouple size on heat flux accuracy will be investigated.

To verify the functionality of both thermocouple types, identical steel platens were instrumented with ribbon and eroding type thermocouples. The platens were placed in the impulse drying simulator, heated to 204°C and brought into contact with a 22°C cold steel platen for 20 ms at a peak pressure of 6.2 MPa. The resulting heat flux versus time curves were then compared to each other and to a readily available theoretical solution as shown in Figure 13.

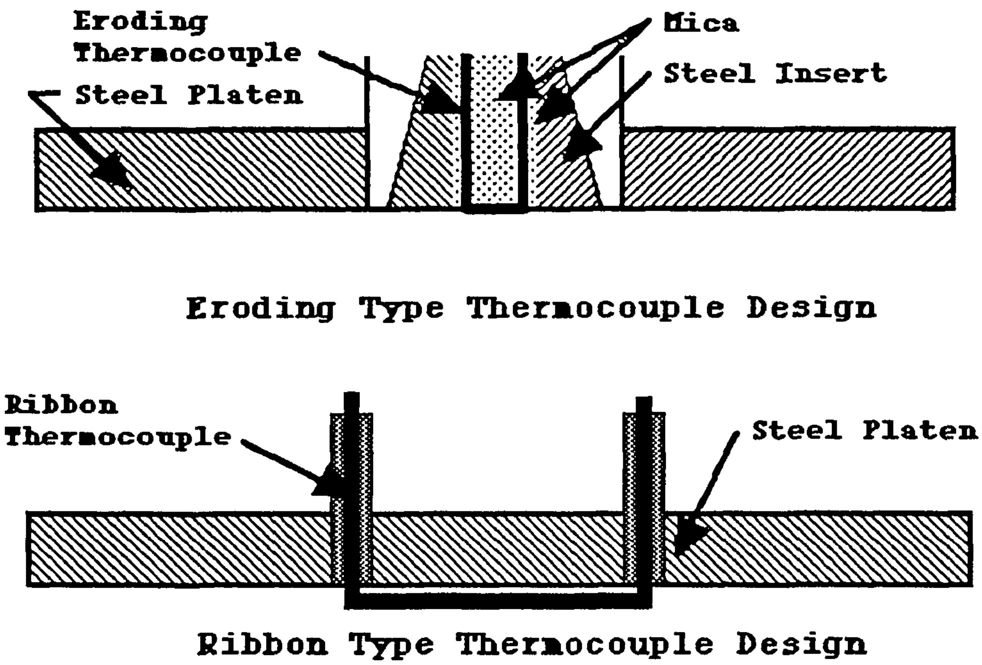

Figure 12: Platen Surface Thermocouple Types

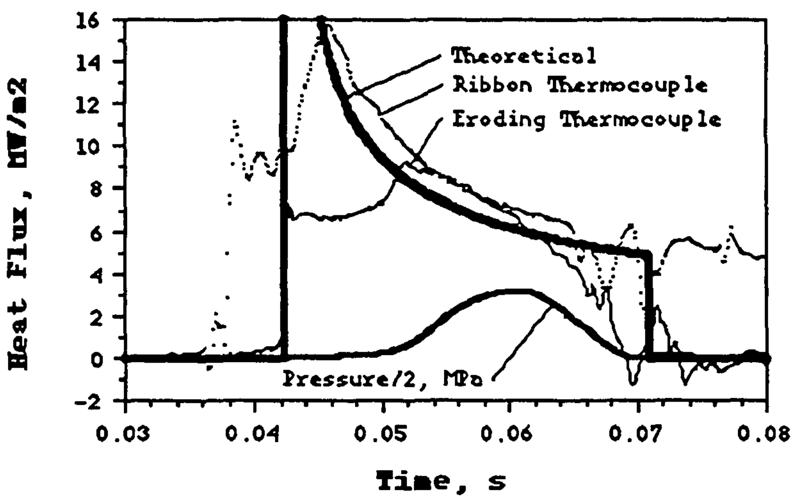

Figure 13: Heat flux curves resulting from contacting a 204°C steel platen onto a 22°C cold steel platen for 20 ms at a peak pressure of 6.2 MPa. Comparison of results from two thermocouple designs and a theoretical solution.

It was observed that, in the pressure pulse interval, both measured heat fluxes agree with the theoretical heat flux. However, it was noted that the measured heat flux from the two thermocouple types diverge during pre-contact and post-contact. The eroding type tends to underestimate heat flux during pre-contact, while the ribbon type overestimates heat flux during post-contact. An explanation for the high post-contact heat flux from the ribbon is that the ribbon is not attached to the steel surface and may pull away from that surface during the opening of the nip. The low initial heat flux from the eroding thermocouple may be due to poor initial contact resulting from non-parallel surfaces. While it would be preferable to have accurate measurements of pre- and post-contact heat transfer, heat transfer during the pressure pulse is of most interest in determination of energy transfer during impulse drying.

Based on calculations reported by Orloff (14), 8% yttrium stabilized zirconium oxide was chosen as the optimum ceramic coating material. Samples of plasma-sprayed yttrium stabilized zirconium oxide, produced in a range of volume fraction from 0.05 to 0.20, were sent to Properties Research Laboratory of West Lafayette, Indiana for testing. Specific heat and thermal diffusivity were measured as a function of temperature and correlated with the measured void volume to predict the specific heat and thermal diffusivity of the ceramic at a theoretical void volume of zero. These results are shown in Figure 14 and Figure 15. The best fit of the data occurred when the correlation constant C' was equal to 8.52.

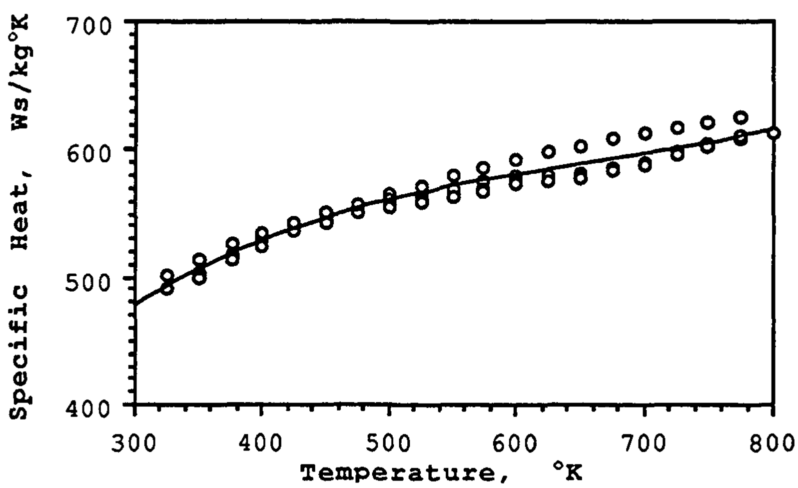

Figure 14: Specific heat of 8% yttrium stabilized zirconium oxide at zero void volume as a function of temperature.

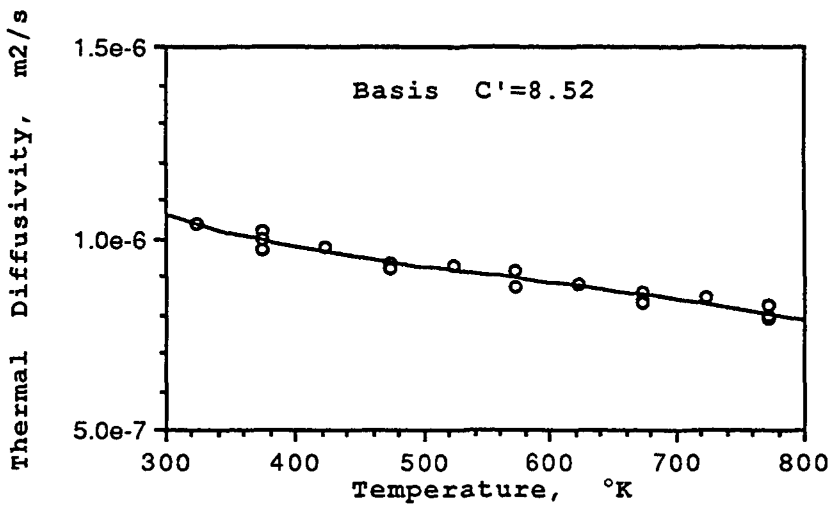

Figure 15: Thermal diffusivity of 8% yttrium stabilized zirconium oxide at zero void volume as a function of temperature.

Orloff (14) hypothesized that sheet delamination could be avoided by reducing the thermal mass of the impulse drying press surface. Thermal mass is defined as the ratio of the thermal conductivity to the square root of the thermal diffusivity. Thermal mass, K, can also be expressed in terms of the density, ρ; specific heat, C_p; and thermal diffusivity, α, of the solid ceramic and the void volume, V, of the coating.

$$K = \left[\rho C_p \sqrt{\alpha}\right]_{solid} \left\{\frac{1-V}{1+C'V}\right\}^{\frac{1}{2}}$$

where the solid, zero void volume density was taken as $\rho = 5500$ kg/m^3.

Figure 16 shows that the thermal mass decreases with increasing void volume while being a weak function of temperature.

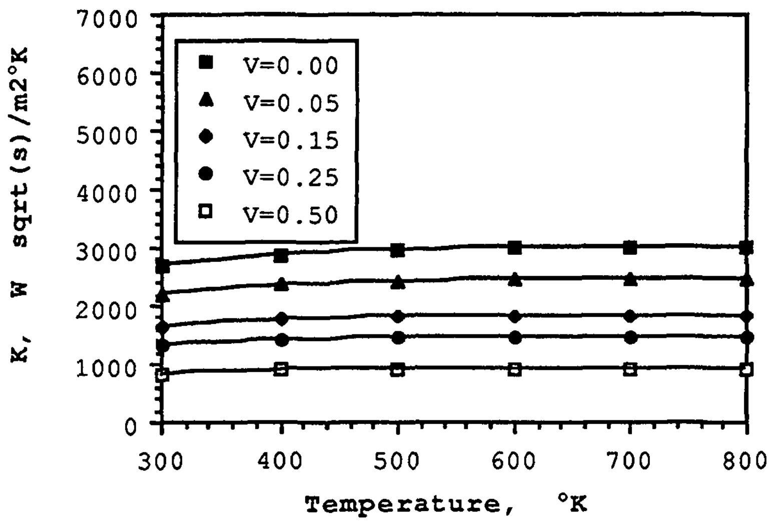

Figure 16: Thermal mass of 8% yttrium stabilized zirconium oxide as a function of void volume and temperature.

To minimize sheet delamination a press roll coating should have the following characteristics:

1. It should have as low a value of K as practical.

2. It should be designed to resist spalling due to mismatch of coating and the base roll thermal expansion coefficients.

3. Its surface should be sealed to prevent steam vapor venting and absorption.

4. Its surface should also provide a low surface energy to minimize sticking.

With these requirements in mind, a prototype press coating was developed in a joint research program among IPST, Fisher-Barton Company and Sandia National Laboratory, funded through a grant from the U.S. Department of Energy.

Fisher-Barton fabricated the prototype coating. A roughened steel surface was coated with a 0.11 mm nickel chromium bond coat, a 0.38 mm 0.15 void volume zirconium oxide-8% yttrium oxide layer, and an as-ground 0.05 mm 0.07 void volume zirconium oxide-8% yttrium oxide outer layer. Once received, the platen was coated with a sealant and high-temperature polymeric release agent.

For the purpose of heat flux calculations, the properties of the coating were taken at a void volume of 0.10.

Experimental Results

Using the described experimental methods, an impulse drying simulation was conducted to compare the performance of the prototype zirconium oxide platen to a steel platen. A 58% yield southern unbleached softwood kraft was refined to 650 ml CSF and was formed into 205 gsm handsheets. The five-inch diameter handsheets were impulse dried from an ingoing sheet temperature of 85°C and an ingoing solids of 30%. To investigate the effect of ingoing moisture gradients, experiments were performed with and without the radiation shield. Both platens were coated with the polymeric release agent so that differences in release would not influence the results.

At a constant dwell time of 20 ms, the handsheets were impulse dried at peak pressures of 3.1 and 6.2 MPa, over a range of initial platen temperatures from 85°C to 500°C. Data acquired at a platen surface temperature of 85°C was used as the wet pressing baseline. Figures 17 and 18 show water removal, expressed as a moisture ratio change, for the steel and the prototype zirconium oxide coated platen at 3.1 and 6.2 MPa where the radiation shield was not in use. A curve fit from previously published data, Orloff(14), is included for comparison. In agreement with the previous findings, water removal was found to be insensitive to platen material at a given initial platen surface temperature and peak pressure.

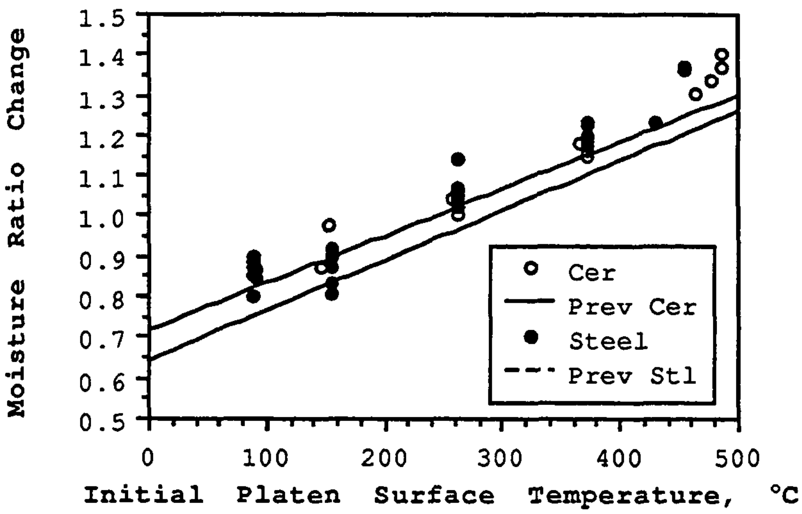

Figure 17: Moisture ratio change for impulse drying of 205 gsm linerboard with steel and prototype ceramic coated platens as a function of initial platen surface temperature. Dwell time = 20 ms, peak pressure = 3.1 MPa, ingoing sheet temperature = 85°C, ingoing solids = 30%, without radiation shield.

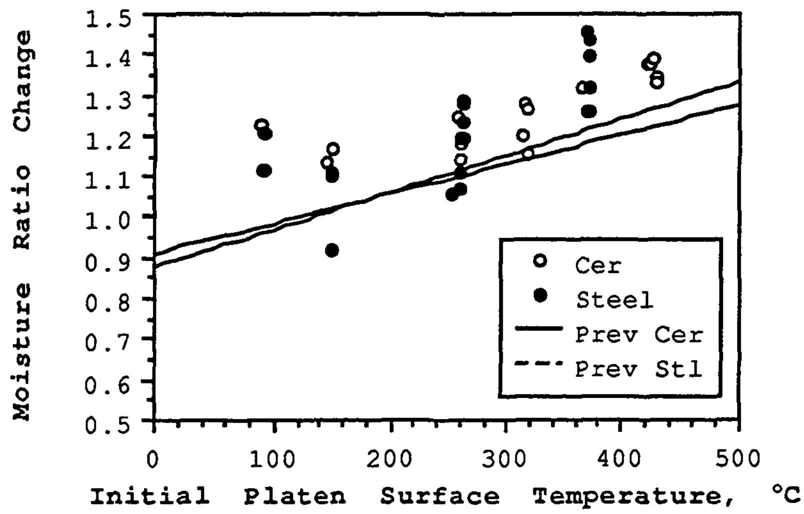

Figure 18: Moisture ratio change for impulse drying of 205 gsm linerboard with steel and prototype ceramic coated platens as a function of initial platen surface temperature. Dwell time = 20 ms, peak pressure = 6.2 MPa, ingoing sheet temperature = 85°C, ingoing solids = 30%, without radiation shield.

Figures 19 and 20 show water removal, expressed as a moisture ratio change, for the steel and the prototype zirconium oxide coated platen at 3.1 and 6.2 MPa where the radiation shield was in use. Again, water removal was found to be insensitive to platen material.

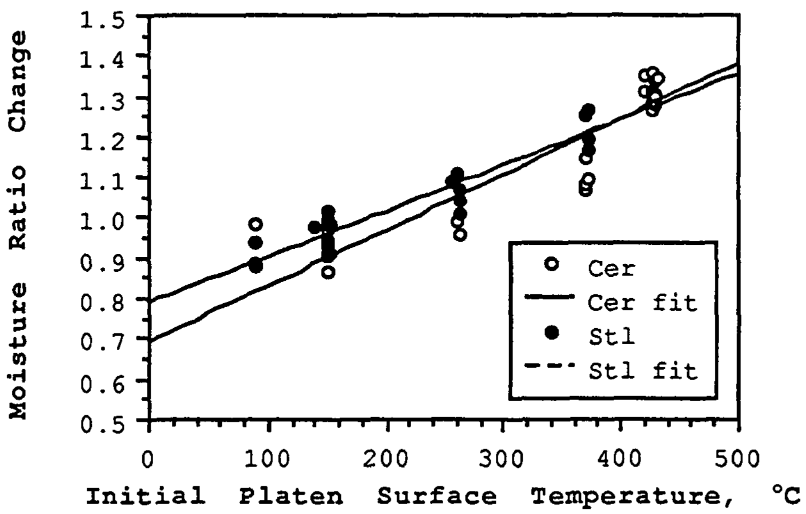

Figure 19: Moisture ratio change for impulse drying of 205 gsm linerboard with steel and prototype ceramic coated platens as a function of initial platen surface temperature. Dwell time = 20 ms, Peak Pressure = 3.1 MPa, Ingoing sheet temperature = 85°C, ingoing solids = 30%, using the radiation shield.

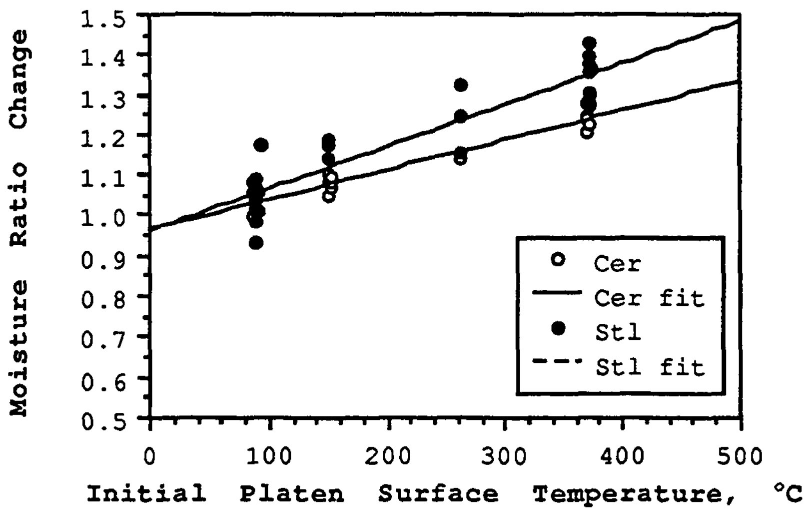

Figure 20: Moisture ratio change for impulse drying of 205 gsm linerboard with steel and prototype ceramic coated platens as a function of initial platen surface temperature. Dwell time = 20 ms, peak pressure = 6.2 MPa, ingoing sheet temperature = 85°C, ingoing solids = 30%, using the radiation shield.

The out-of-plane specific elastic modulus has been shown to be proportional to standard destructive strength tests such as the STFI compressive strength (12). Analysis of non-delaminated samples showed that the specific elastic modulus was a function of sheet density and independent of platen material, as shown in Figure 21. In previous work, Orloff(14) obtained higher elastic modulus vs. density curves for steel as compared to that from the prototype ceramic coated platen. A probable explanation is that present work was processed in small batches of steel experiments followed by ceramic experiments, while the previous work was done in a consecutive manner. Hence, previous work may have been slightly biased by uncontrolled variables.

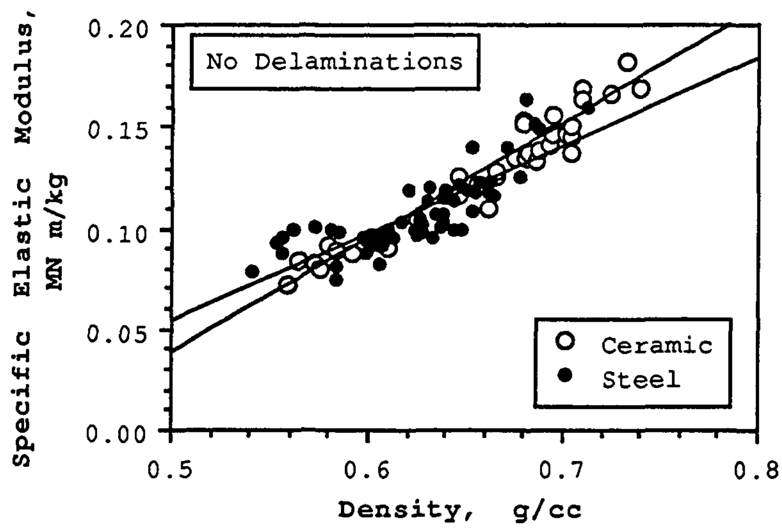

Figure 21: Specific elastic modulus for impulse drying of 205 gsm linerboard as a function of soft platen density for steel and prototype zirconium oxide platens. Dwell time = 20 ms, ingoing sheet temperature = 85°C, ingoing solids = 30%.

As has been demonstrated by Crouse (7), sheet delamination limits the operating temperature of impulse drying roll surfaces and, consequently, limits water removal. Hence, to evaluate potential roll surfaces, the key performance variables are water removal and delamination control. With this in mind, a performance map showing the coefficient of variation of the specific elastic modulus vs. moisture ratio change was found to be useful. Comparative performance maps for each of the peak pressures investigated are shown in Figures 22, 23, 24 and 25. Also shown are fitted equations to the data. Based on the intersection of the fitted curves and the 10% delamination criteria line, a maximum moisture ratio change could be determined for each platen type at each condition. At all conditions, the steel platen resulted in excessively high coefficients of variation at fairly low values of moisture ratio change.

The performance of the zirconium oxide surface was consistently superior.

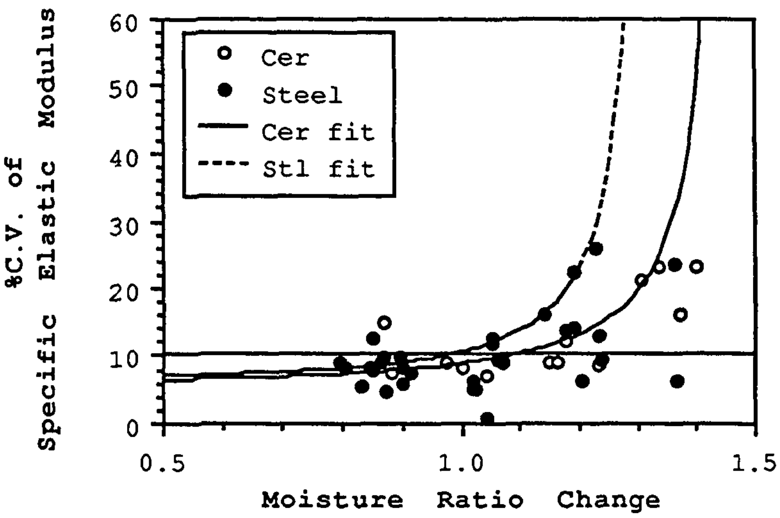

Figure 22: Coefficient of variation of specific elastic modulus as a function of moisture ratio change for impulse drying of 205gsm linerboard with steel and with the prototype ceramic coated platens at a peak pressure of 3.1 MPa without the radiation shield. Dwell time=20ms, impulse=0.028 MPas, ingoing sheet temperature=85°C, ingoing solids=30%.

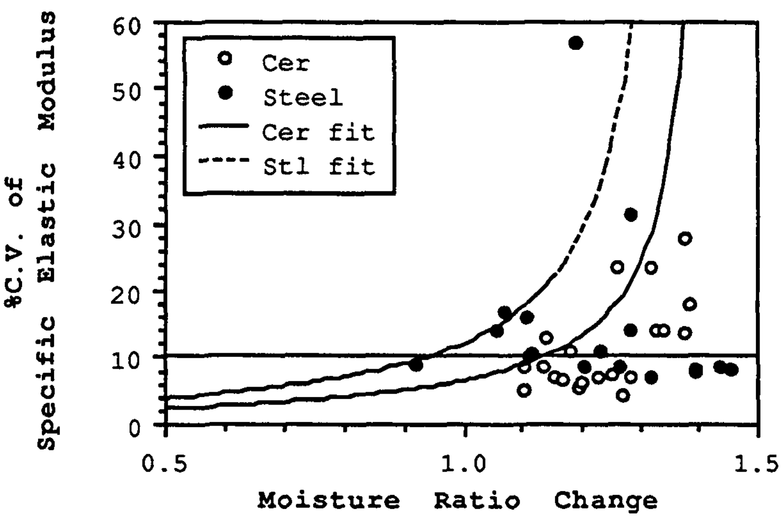

Figure 23: Coefficient of variation of specific elastic modulus as a function of moisture ratio change for impulse drying of 205gsm linerboard with steel and with the prototype ceramic coated platens at a peak pressure of 6.2 MPa without the radiation shield. Dwell time=20ms, impulse=0.062 MPas, ingoing sheet temperature=85°C, ingoing solids=30%.

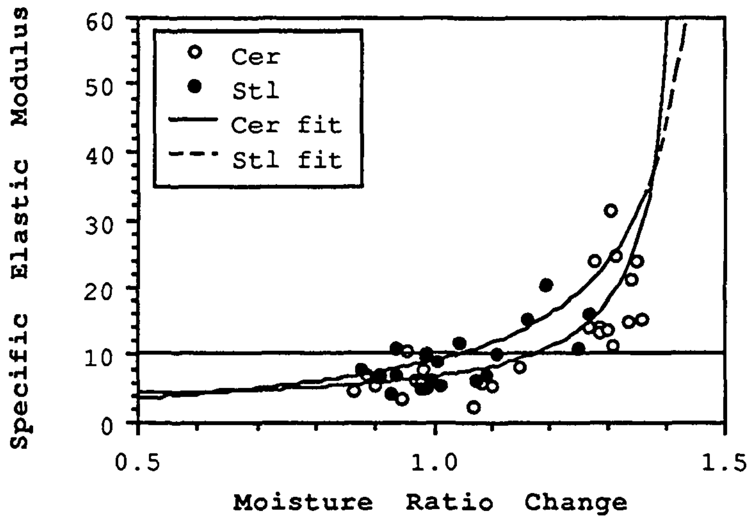

Figure 24: Coefficient of variation of specific elastic modulus as a function of moisture ratio change for impulse drying of 205gsm linerboard with steel and with the prototype ceramic coated platens at a peak pressure of 3.1 MPa with the radiation shield. Dwell time=20ms, impulse=0.028 MPas, ingoing sheet temperature=85°C, ingoing solids=30%.

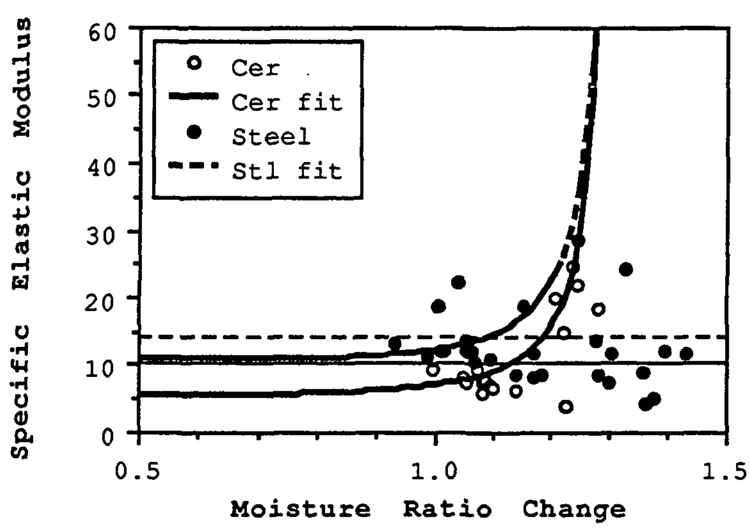

Figure 25: Coefficient of variation of specific elastic modulus as a function of moisture ratio change for impulse drying of 205gsm linerboard with steel and with the prototype ceramic coated platens at a peak pressure of 6.2 MPa with the radiation shield. Dwell time=20ms, impulse=0.062 MPas, ingoing sheet temperature=85°C, ingoing solids=30%.

The platen surface temperature, measured as a function of time during impulse drying, was used to calculate instantaneous heat flux during the impulse drying event. These curves were then integrated from the instant of first pressure rise to the instant of pressure reducing to zero. The integral represents the energy transferred to the sheet during the impulse drying process. Figures 26 and 27 show energy transfer as a function of initial platen surface temperature for the steel and prototype ceramic-coated platens, with and without the radiation shield for both high and low peak pressures.

These curves clearly show the differences inherent in impulse drying with the two materials. With steel as the press surface, energy transfer to the sheet is non-linear and dependent on peak pressure as well as initial platen surface temperature. With the prototype ceramic coating as the press surface, energy transfer is linear with initial platen surface temperature and is independent of peak pressure. As pressure can only effect the thermal properties of the sheet being impulse dryed, these results suggest that the sheet controls heat transfer for the steel platen. In contrast, the state of the sheet has no influence on heat transfer when the prototype ceramic coating is used.

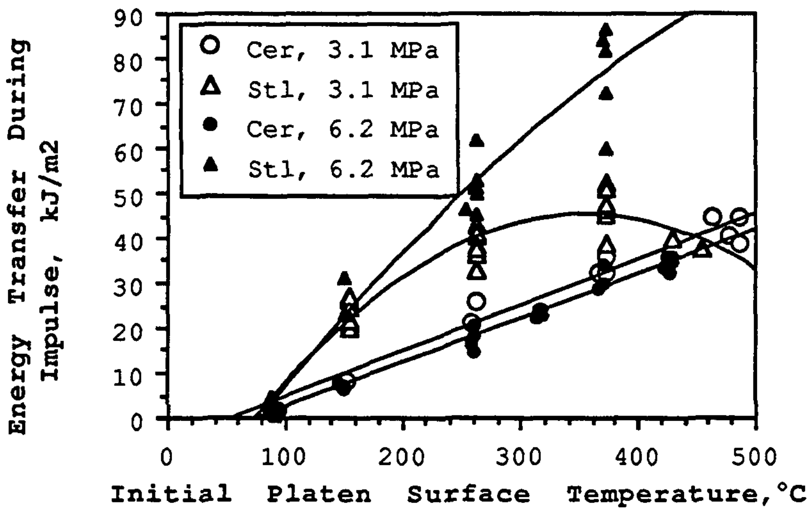

Figure 26: Energy transfer during impulse drying as a function of initial platen surface temperature for impulse drying 205gsm linerboard with steel and with the prototype ceramic-coated platens without the radiation shield. Dwell time=20ms, ingoing sheet temperature=85°C, ingoing solids=30%.

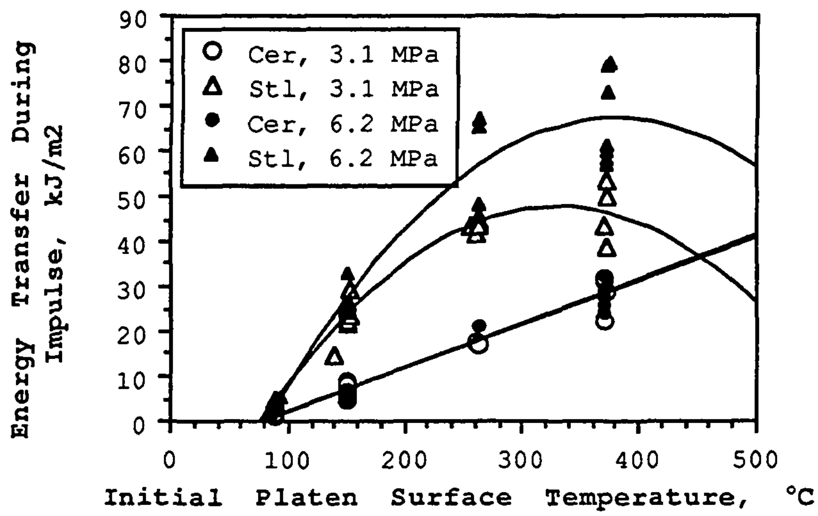

Figure 27: Energy transfer during impulse drying as a function of initial platen surface temperature for impulse drying 205gsm linerboard with steel and with the prototype ceramic-coated platens with the radiation shield. Dwell time=20ms, ingoing sheet temperature=85°C, ingoing solids=30%.

In order to compare and contrast the influence of platen type, ingoing moisture gradients and peak pressure on impulse drying, the results of the experiments have been tabulated in Tables 1, 2 and 3. Table 1 identifies the experimental conditions that were investigated by case number.

TABLE 1

EXPERIMENTAL CONDITIONS

CASE	PLATEN	RADIATION SHIELD	PEAK PRESSURE MPa
1	steel	no	3.1 MPa
2	steel	yes	3.1 MPa
3	steel	no	6.2 MPa
4	steel	yes	6.2 MPa
5	ceramic	no	3.1 MPa
6	ceramic	yes	3.1 MPa
7	ceramic	no	6.2 MPa
8	ceramic	yes	6.2 MPa

Table 2 shows the moisture ratio change that can be achieved through single felted wet pressing at an initial platen surface temperature of 88°C for each case. In addition, the soft platen density, specific elastic modulus and measured energy transfer are reported. In increasing the peak pressure, the impulse increases resulting in an increase in water removal, density and sheet strength.

TABLE 2

WET PRESSING AT AN INITIAL PLATEN SURFACE TEMPERATURE OF 88°C

CASE	WET PRESSING MOIST. RATIO CHANGE	Soft Platen Density, g/cc	Specific Elastic Modulus, MN m/kg	Energy Transfer, kJ/m^2
1	0.78	.568	.088	3.6
2	0.89	.583	.081	3.7
3	0.89	.675	.128	2.2
4	1.05	.649	.118	2.3
5	0.81	.591	.101	3.0
6	0.81	.562	.077	1.1
7	1.06	.680	.145	0.9
8	1.03	.669	.127	0.3

Table 3 shows the maximum moisture ratio change and corresponding initial platen surface temperature determined from the performance curves shown in Figures 22 through 25. Corresponding soft platen density and specific elastic modulus are also tabulated. Measured energy transfer and incremental energy use are also presented.

Incremental energy use was defined as the difference in energy transfer between impulse drying and wet pressing, divided by the difference in water removal. Incremental energy use quantifies the energy required to remove a kilogram of water beyond what can be achieved by single felted wet pressing.

Stepwise regression of the tabulated data shows that the maximum moisture ratio change improves when impulse drying was accomplished with the prototype ceramic-coated platen and when the radiation shield was in use. Increased soft platen density and elastic modulus were achieved by using the prototype ceramic-coated platen and by increasing the peak pressure of the impulse drying process. Use of the prototype ceramic coated platen and increased peak pressure results in a reduction in energy transfer to the sheet. Incremental energy use is entirely a function of platen type and is substantially reduced through use of the prototype ceramic coating.

To help put the incremental energy use numbers in perspective, conventional evaporative drying would require 2257 kJ/kg as compared to 666 kJ/kg for impulse drying with the prototype ceramic coating.

TABLE 3

IMPULSE DRIED PROPERTIES AT MAXIMUM MOISTURE RATIO CHANGE

CASE	MAX. MOIST. RATIO CHANGE	Initial Platen Surface Temp, °C	Soft Platen Density, g/cc	Specific Elastic Modulus, MN m/kg	Energy Transfer, kJ/m^2	Incremental Energy Use kJ/kg
1	0.98	220	.615	.106	34.4	744
2	1.04	225	.627	.105	39.2	1113
3	0.94	119	.671	.126	12.1	926
4	1.09	122	.673	.131	16.6	1924
5	1.09	290	.660	.135	24.0	375
6	1.17	350	.642	.114	26.3	341
7	1.14	183	.693	.154	10.4	576
8	1.13	226	.708	.145	14.2	666

PILOT EVALUATION OF THE PROTOTYPE ROLL

Experimental Methods

Overview and Objectives

The prototype ceramic-coated press roll was installed on the first nip of the pilot impulse dryer as shown on Figure 28. In order to control the ingoing surface temperature of the roll, an infrared sensor was also installed. In addition, a steam box in combination with a vacuum box were used to preheat the web prior to introduction into the first press nip. The steam box was instrumented with a temperature- and pressure-compensated vortex flow meter to record steam mass flow rate. The temperature and pressure just prior to exiting the box were also recorded along with the vacuum box operating pressure.

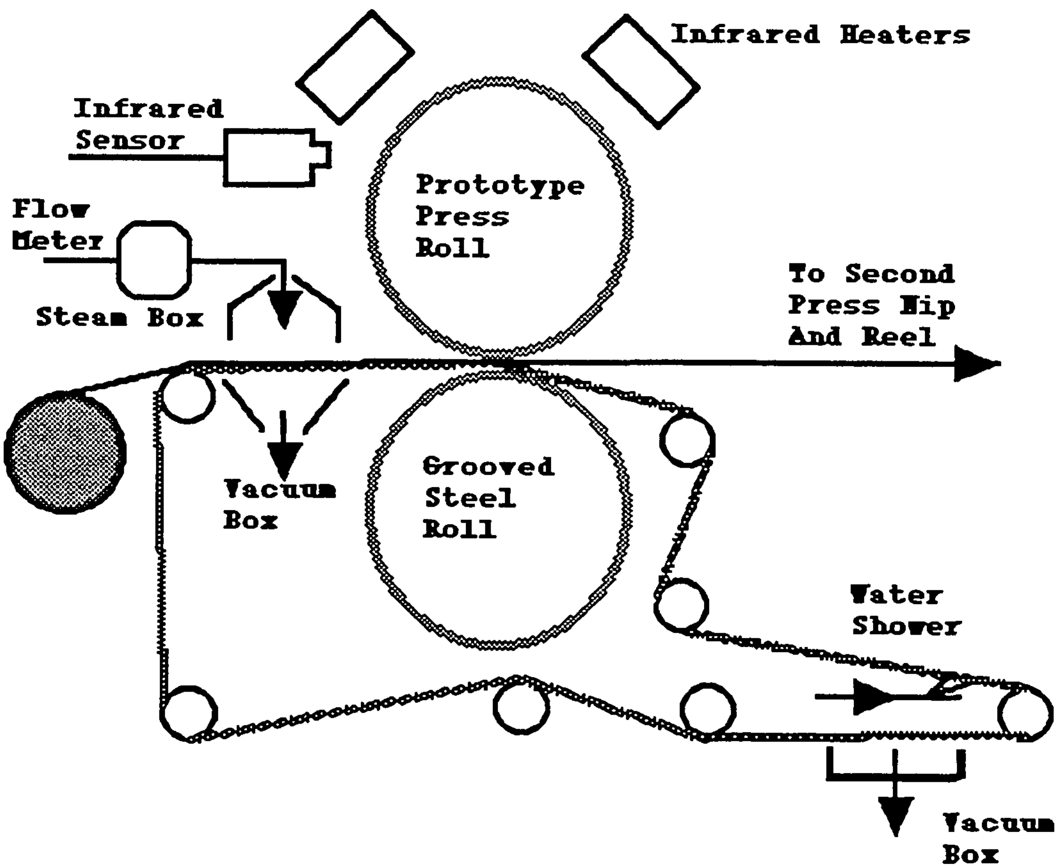

Figure 28. First nip of the pilot-scale two-nip impulse dryer.

Forty-two pound liner (205 gsm) was made from an unbleached softwood kraft refined to 650 ml CSF. In order to achieve a range of ingoing solids from 30 to 50%, the linerboard was formed on the IPST web former, unwound and cold pressed on the second nip of the pilot dryer to the desired dryness level.

As steam preheating adds water to the sheet, a series of experiments was performed to quantify this effect over a range of ingoing solids.

In a series of impulse drying experiments, the first nip was set to a peak pressure of 6.2 MPa. Nip impressions demonstrated that the pressure distribution across the width of the prototype press roll was uniform and accurate. Based on a measured nip width of 20 mm at 6.2 MPa, a dryer speed of 60 m/min corresponded to a dwell time of 20 ms, while a dryer speed of 30 m/min corresponded to a dwell time of 40 ms.

In order to demonstrate the benefit of impulse drying over single felted wet pressing, drying experiments were conducted over a range of ingoing roll surface temperatures from 100°C to 430°C. Experiments were conducted over a range of ingoing solids from 30% to 45% at both 20 ms and 40 ms.

Raw Materials and Refining

The pulp used in these experiments was an unbleached southern softwood kraft bottom sheet linerboard pulp collected from the last stage washers. The Kappa number ranged from 65 to 69 depending on the batch.

Carbohydrate chemical composition was typically 79.4% glucose, 7.4% xylose, 6.9% mannose, 0.6% arabinose and 0.4% galactose.

Each batch was received from the mill in 208-liter drums. To insure uniformity, all of the drums of pulp from a given batch were processed at the same time. The pulp was washed to remove residual black liquor. Upon completion of washing, the pulp was refined on a 2.3 kg Valley beater. The beater was repeatedly charged with 9.5 kg of washed pulp, diluted with tap water to a 2 % consistency and beaten to 650 ml CSF. Beating times were typically 39.7 minutes to achieve 650 ml CSF.

The beaten pulp was pumped into a fine mesh screen box for dewatering and centrifuged to 25% solids. After fluffing and blending, the pulp was placed in double lined plastic bags for storage in the cooler at a temperature of 4°C.

Fiber length distributions were measured after refining and fluffing and after sheet formation. As shown in Figure 29, the as-received pulp had a number weighted average length of 1.43 mm. Refining the pulp to 650 ml CSF reduced the number weighted average fiber length to 1.35 mm after fluffing. As some fines were lost during sheet formation, the number weighted average length in the formed sheet was 1.57 mm.

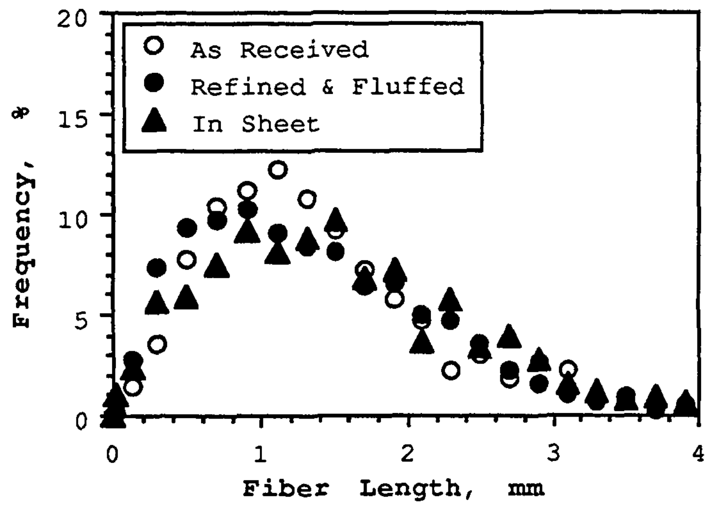

Figure 29: Fiber length distribution as received, after refining to 650 ml CSF, and as found in sheet formed from the refined pulp as measured by projection.

Sheet Formation and Pressing

Paper was typically produced one week prior to scheduled impulse drying experiments. Previously refined and fluffed pulp was removed from the cooler and disintegrated with tap water for five minutes, under no load, in the Valley beater. The pulp was pumped to a 570-liter stock chest where tap water was added to obtain a consistency of 1.2 %. While maintaining the stock chest consistency, additional pulp was disintegrated and pumped to the stock chest until the chest was full.

The pulp was circulated through the head tank via the stock pump. A pulp sample was collected at the head tank for pH and consistency measurements. A 10% solution of alum (aluminum sulfate) was added to the stock chest to achieve a pH of 5.5 to 6.0.

To produce 205 gsm single-ply linerboard, the web former was set at a machine speed of 2.3 m/min. The feed pump was set to deliver a mass flow rate of 8 kg/min. The white water return was set to maintain a forming box vacuum of 2.5 cm Hg at a forming box consistency of between 0.15-0.20 percent. The couch press was turned to maximum while the press nip was set between 35 to 100 kPa. The pressure in the steam can was set to between 100 and 170 kPa.

A 3 m section of paper was formed. From basis weight and percent solids measurements, web former operating conditions were then adjusted to achieve the desired basis weight and solids.

When conditions were properly adjusted, a continuous web was formed and reeled onto a 7.6cm x 33 cm core. Each roll was 30 cm wide and about 45 m long. Two rolls could be made from a full stock chest. The percent solids at the reel was typically between 25 and 30 percent.

When required, the pilot impulse dryer was used to press the web to achieve higher percent solids. The second press nip was used since the polymer release coating, applied to the first nip ceramic roll, was sensitive to liquid water when the roll was cold. The press was run at a speed of 3 to 5 m/min. The vacuum system was used to dry the felt during pressing. The nip load was varied depending on the end condition desired. If 42% solids was required, the nip loading was set at 9,000 N. To achieve 50% solids, the nip loading was set at 11,000 N and the web was run through the press three times.

To characterize the pressed sheet, samples were taken and tested for Kappa number, fiber length distribution and out-of-plane permeability. Typical out-of plane permeability results for 42% solids are shown in Figure 30.

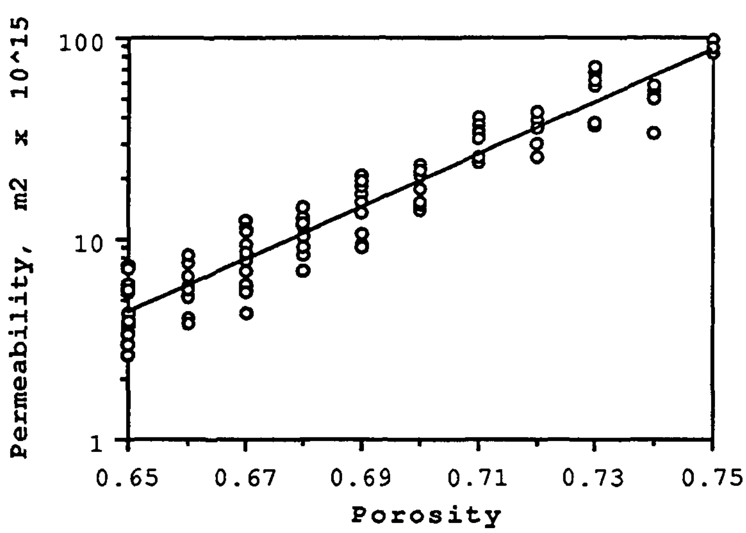

Figure 30: Sheet permeability as a function of sheet porosity for 205 gsm single-ply linerboard formed from unbleached softwood kraft refined to 650 ml CSF and pressed to 42% solids.

Impulse Drying Experimental Procedures

After obtaining the appropriate dryness, paper made on the web former was placed on the unwind stand of the pilot impulse dryer and preparations were made for wet pressing and impulse drying. Five major variables were set for each run. These were press roll temperature, nip load, nip residence time, pre-heat steam mass flow rate and vacuum box pressure.

To prevent the web from sticking to the heated roll during the runs, a release agent was applied to the ceramic roll. The roll was first cleaned using Frekote Poly-Cleaner. With the roll heated to 100°C, several coats of Frekote Mold Sealer B-15 were applied with a clean cotton cloth, followed by three coats of Frekote Mold Release 700-NC. The coatings were allowed to dry for 15 minutes between applications.

The roll contacting the web was set at 106°C for wet pressing runs. Impulse drying runs were conducted at roll surface temperatures ranging from 300°C to 430°C. An infrared pyrometer was used to control the surface temperature of the ceramic coated roll. The pyrometer was positioned just prior to the nip to record the temperature of the roll and to serve as the input to the temperature controller. The controller adjusted the output of the infrared roll heaters to maintain a constant ingoing roll surface temperature. As the thermal demand increased upon closing the nip, the controller would increase the heater output. The controller maintained a constant ingoing roll surface temperature during each experiment.

Peak nip pressure was verified using Fuji prescale LW pressure-sensitive film. The film was calibrated over a range of known pressures, using the laboratory-scale electrohydraulic press. Static nip impressions were then taken on the pilot impulse dryer to provide a measure of peak pressure, nip width and pressure uniformity. Based on these measurements, adjustments were made on the independent hydraulic load cells at each end of the roll to attain a uniform impression across the width of the roll. After balancing, a nip impression was taken and compared to the calibrated impressions. Peak nip pressures were found to be accurately predicted by load cell readings and the measured nip width.

While operating, nip pressure was set, monitored, and adjusted using the digital output load cells. A total load of 18680 N applied to a nip area of 0.006 m^2 results in an average pressure of 3.1 MPa and a peak pressure of 6.2 MPa.

Nip residence times of 20 and 40 ms duration were evaluated in the pilot-scale experiments. With a nip width of 0.02m, the machine speeds necessary to achieve these durations were 60 and 30 m/min, respectively. The controller was set for these speeds. Paper was threaded into the pilot impulse dryer at 6 m/min with the nip open. After threading, the first nip was closed and the steam and vacuum were turned on. When the paper was threaded onto the reel, the machine speed was increased to the desired run speed by selecting the proper speed potentiometer. The controller would uniformly and quickly bring the machine up to the desired speed and hold that speed until the conclusion of the run.

Prior to entering the nip, the ingoing web was preheated by injecting steam through the sheet and felt. A steam box and vacuum box were used for this purpose. Conditions were set to preheat the sheet to 100°C.

The primary variable controlling preheat temperature was the source pressure of the steam, which was set to 250kPa. Under these conditions, the temperature of the steam entering the steam box was 110°C, the pressure in the steam box was 180KPa, and the steam mass flow rate was 214 to 230 kg/hr. A vacuum box, positioned directly below the steam box and under the sheet and felt, drew a vacuum of 25 cm Hg.

Calculations have shown that steam preheating the web at the above conditions resulted in ingoing sheet temperatures of 100°C. To verify this, thermocouples were placed between the sheet and felt to record sheet temperature during steam preheating. The results confirmed that, over the range of speeds and ingoing solids of these experiments, sheet temperatures were preheated to between 90°C and 100°C.

As steam preheating adds water to the sheet, calibration experiments were conducted to measure the change in sheet solids due to steam preheating. Water gain from steam preheating was found to be independent of freeness and speed. Typically, sheets experienced a 1% drop in dryness due to steam preheating. All reported ingoing solids have been corrected to reflect the dryness of the sheet entering the impulse dryer.

Felt conditioning was achieved by spraying water on both sides of the felt following the nip. Excess water was pulled from the felt using a 30 cm Hg vacuum. This washed and cooled the felt and provided a consistent felt moisture ratio of 0.15 to 0.20.

It has been suggested that felt permeability may be a contributing variable to impulse drying. In this regard, the Frazier air permeability of felts was measured before a felt was installed on the pilot dryer and was also measured when the felt was removed after completion of impulse drying experiments. Testing was conducted at the Southern College of Technology. Frazier air permeability was measured in cubic meters of air drawn through the felt per square meter of felt surface per minute. New felts that had not been conditioned had a permeability of about 7 m^3/m^2 min. After conditioning, permeability decreased to about 4.5 m^3/m^2 min. After pilot-scale impulse drying experiments were completed, felts were found to have permeabilities as low as 1.4 m^3/m^2 min. While felt air permeability decreased with use, the felts were believed to be functional when they were removed.

Experimental Results

A preliminary set of experiments was performed with the pre-heat steam flow rate set at 214 kg/h. The results of that experiment are shown in Figures 31 through 37. At a nip residence time of 40 ms and at an ingoing sheet dryness of 41% solids, outgoing dryness of 60% solids could be achieved when the ingoing roll surface temperature was raised to 371°C. This was a 6% solids improvement over wet pressing, as shown in Figure 31. At a nip residence time of 20 ms only a slight improvement over wet pressing was realized.

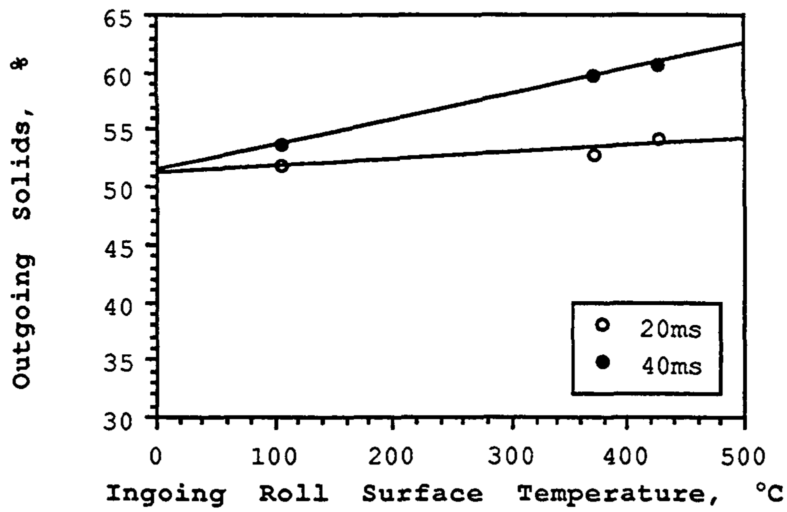

Figure 31: Outgoing solids as a function of ingoing roll surface temperature for the pilot-scale impulse drying of 205 gsm linerboard with the prototype ceramic-coated press roll at nip residence times of 20 and 40 ms. Ingoing solids=41%, ingoing sheet temperature=100°C, peak pressure=6.2MPa.

The objective was to assess whether the prototype ceramic-coated press roll could be used to impulse dry heavyweight grades without inducing sheet delamination. To characterize the physical properties of the paper, samples of the wet pressed and impulse dried paper were finish dried on a drum dryer, conditioned to TAPPI standards and tested. Figure 32 shows the location of various tests performed on 22 cm x 28 cm samples. Sixty locations per sheet were tested by out-of-plane ultrasound and by STFI compression tests. In addition, three locations per sheet were tested for burst strength.

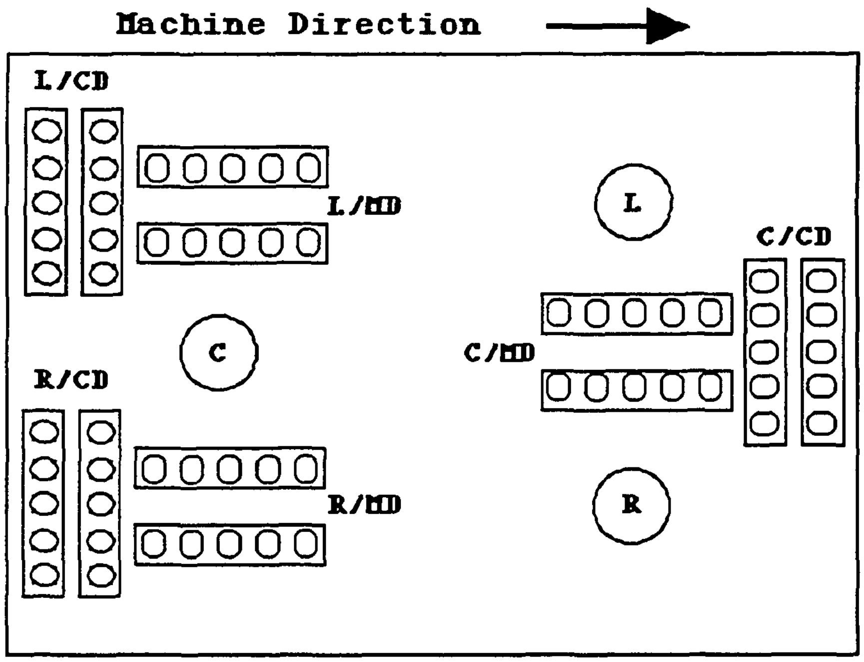

Figure 32. Schematic of sheet test locations.

As in laboratory-scale work, delaminated regions of a sheet typically had a lower out-of-plane specific elastic modulus than surrounding non-delaminated regions of the sheet. Hence, the coefficient of variation of the out-of-plane specific elastic modulus was used to detect the onset of sheet delamination. By comparing the coefficient of variation of impulse dried samples with that of wet pressed samples, delamination was detected.

Figure 33 shows the sheet average coefficient of variation of the out-of-plane specific elastic modulus for the conditions reported in Figure 31. The sheet average coefficient was the average of six coefficients calculated for each 22 cm x 28 cm sheet. For a nip residence time of 20 ms, ingoing roll surface temperatures of as high as 426°C could be operated without inducing sheet delamination. At a nip residence time of 40 ms, delamination was not detected at an ingoing roll surface temperature of 371°C but was present at 426°C. To further validate this observation, samples from each condition were frozen, fractured and cross sections analyzed using a scanning electron microscope. The micrographs confirmed the conclusions reached via the ultrasonic measurements.

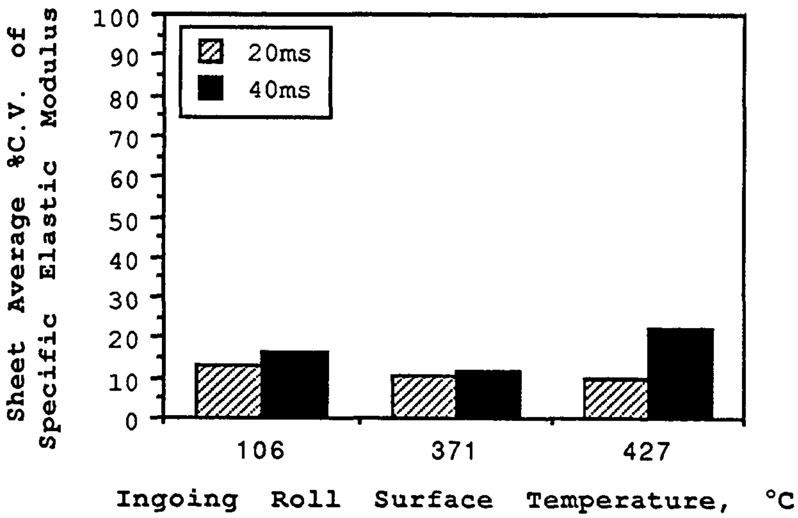

Figure 33: Sheet average %C.V. of specific elastic modulus as a function of ingoing roll surface temperature for the pilot-scale impulse drying of 205 gsm linerboard with the prototype ceramic-coated press roll at nip residence times of 20 and 40 ms. Ingoing solids=41%, ingoing sheet temperature=100°C, peak pressure=6.2MPa.

Out-of-plane specific elastic modulus, burst index and STFI compression index each give an indication of sheet strength. To demonstrate the improvement in physical properties achievable through impulse drying, each of these properties has been plotted as a function of ingoing roll surface temperature.

As shown in Figure 34, a substantial improvement in out-of-plane specific elastic modulus was achieved at a nip residence time of 40 ms.

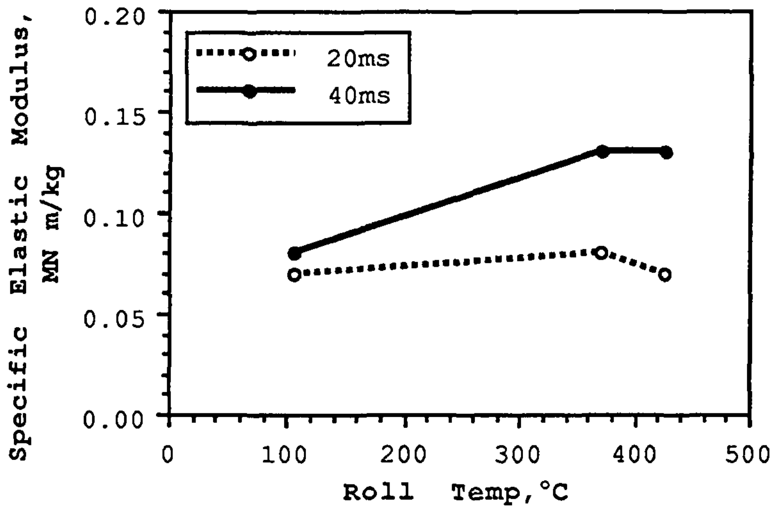

Figure 34: Specific elastic modulus as a function of ingoing roll surface temperature for the pilot-scale impulse drying of 205 gsm linerboard with the prototype ceramic-coated press roll at nip residence times of 20 and 40 ms. Ingoing solids=41%, ingoing sheet temperature=100°C, peak pressure=6.2MPa.

Soft platen density, measured during the ultrasonic testing and shown in Figure 35, also improved through impulse drying at a nip residence time of 40 ms. Notice the decrease in density at 427°, which is characteristic of delamination.

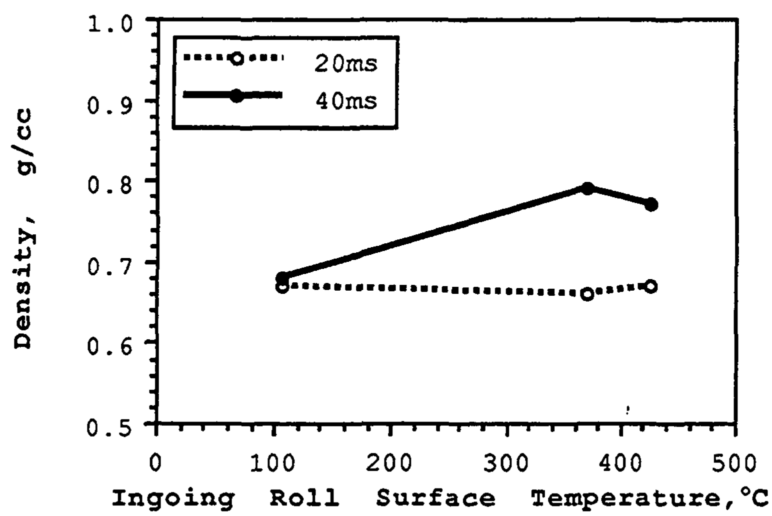

Figure 35: Soft platen density as a function of ingoing roll surface temperature for the pilot-scale impulse drying of 205 gsm linerboard with the prototype ceramic-coated press roll at nip residence times of 20 and 40 ms. Ingoing solids=41%, ingoing sheet temperature=100°C, peak pressure=6.2MPa.

As shown in Figure 36, burst index was enhanced by impulse drying at nip residence times of both 20 and 40 ms.

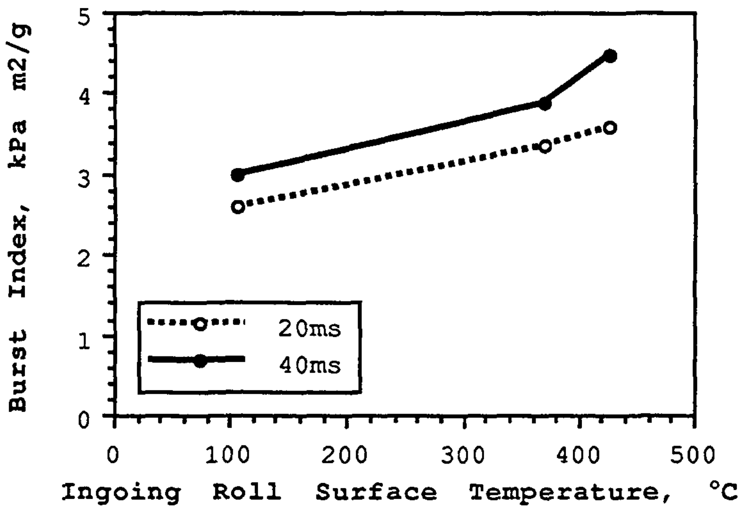

Figure 36: Burst index as a function of ingoing roll surface temperature for the pilot-scale impulse drying of 205 gsm linerboard with the prototype ceramic-coated press roll at nip residence times of 20 and 40 ms. Ingoing solids=41%, ingoing sheet temperature=100°C, peak pressure=6.2MPa.

Figure 37 shows both machine direction (MD) and cross direction (CD) STFI index as a function of ingoing roll surface temperature. As in the case of elastic modulus, improvements to STFI index were achieved at a nip residence time of 40 ms.

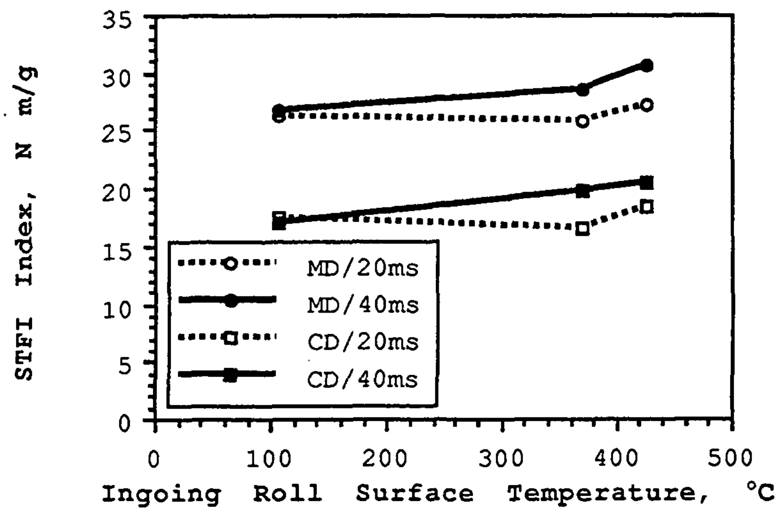

Figure 37: STFI compression index as a function of ingoing roll surface temperature for the pilot-scale impulse drying of 205 gsm linerboard with the prototype ceramic-coated press roll at nip residence times of 20 and 40 ms. Ingoing solids=41%, ingoing sheet temperature=100°C, peak pressure=6.2MPa.

Table 4 summarizes the results of these preliminary experiments in terms of maximum water removal and physical properties achieved for an ingoing solids of 41%. To achieve maximum benefit of impulse drying, nip residence times approaching 40 ms were required.

TABLE 4

SUMMARY OF PRELIMINARY PILOT-SCALE EXPERIMENTS

	WET PRESS 20ms	IMPULSE DRY 427°C 20ms	WET PRESS 40ms	IMPULSE DRY 371°C 40ms
Solids Out, %	52	54	54	60
Modulus, MN m/kg	0.07	0.07	0.07	0.12
Burst Index,kPa m^2/g	2.6	3.5	3.0	4.0
MD STFI Index,N m/g	26	26	26	29
CD STFI Index,N m/g	17	17	17	20

A subsequent set of experiments was run to confirm the findings of the preliminary experiment and to expand the data set to include impulse drying from an ingoing dryness of 34% solids.

In these experiments, the pre-heat steam flow rate was set at 230 kg/h, which was slightly higher than in the preliminary experiment.

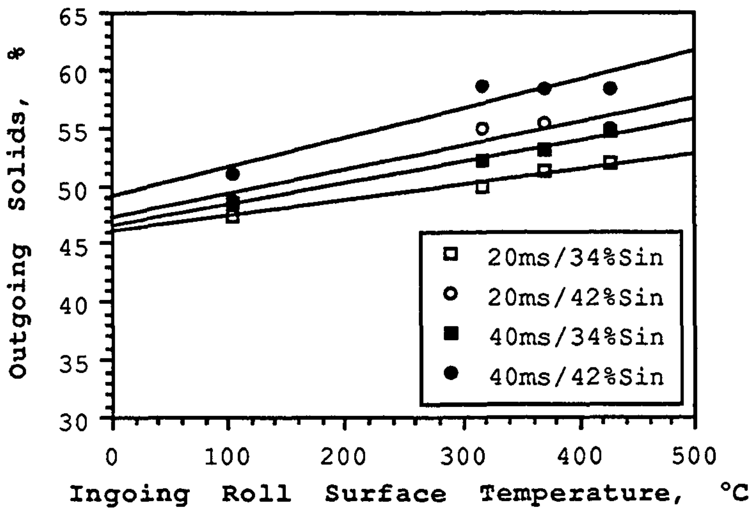

Figure 38: Outgoing solids as a function of ingoing roll surface temperature for the pilot-scale impulse drying of 205 gsm linerboard with the prototype ceramic-coated press roll at nip residence times of 20 and 40 ms and ingoing solids of 34 and 42%. Ingoing sheet temperature=100°C, peak pressure=6.2MPa.

Figure 38 shows outgoing solids as a function of ingoing roll surface temperature. The results confirm the results of the preliminary pilot experiments, in that an improvement in outgoing solids of 6% was achieved at an ingoing dryness of 42%. While impulse drying at 20 ms was not as impressive as at 40ms, there was an improvement over wet pressing. As expected, impulse drying from 34% solids resulted in lower outgoing solids than starting from 42%.

Conventional pressing technology is capable of achieving outgoing solids of about 52%. Figure 38 shows that impulse drying can deliver substantially higher dryness when ingoing solids are greater than 40% and nip residence times are 40 ms or more. At a typical paper machine speed of 760 m/min, a 50 cm long press shoe would be required to achieve a 40 ms nip residence time. Hence, the data support the view that the technology requires a long nip press which should be located in the third press position on the paper machine.

Figure 39 shows the sheet average coefficient of variation of the specific elastic modulus for each of the experimental conditions. Using the coefficient for wet pressing as a criterion, sheets were free of delamination at ingoing roll surface temperatures equal to or below 316°C. As in the previous experiment, scanning electron microscopy was used to verify this conclusion. At a roll temperature of 316°C, outgoing solids of 57% was attained at an ingoing dryness of 42% and at a nip residence time of 40 ms.

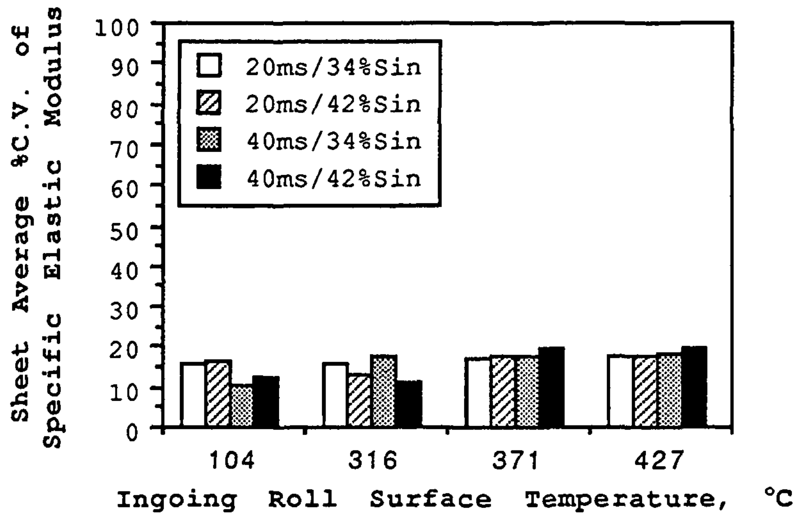

Figure 39: Sheet average %C.V. of specific elastic modulus as a function of ingoing roll surface temperature for the pilot-scale impulse drying of 205 gsm linerboard with the prototype ceramic-coated press roll at nip residence times of 20 and 40 ms and ingoing solids of 34 and 42%. Ingoing sheet temperature=100°C, peak pressure=6.2MPa.

Figures 40 through 44 show specific elastic modulus, soft platen density, burst index and STFI index as a function of ingoing roll surface temperature for each condition. Each of these physical properties increased with increasing ingoing roll surface temperature until about 316°C. At higher temperatures, physical properties tended to decrease as a result of delamination.

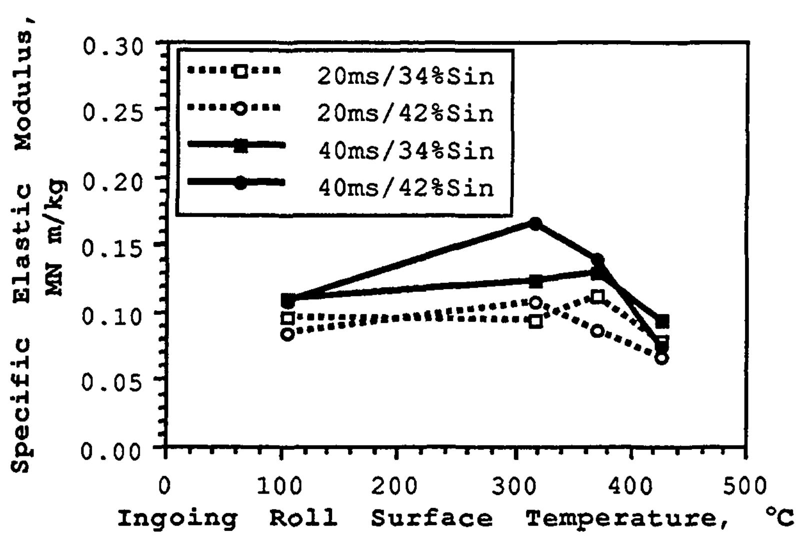

Figure 40: Specific elastic modulus as a function of ingoing roll surface temperature for the pilot-scale impulse drying of 205 gsm linerboard with the prototype ceramic-coated press

roll at nip residence times of 20 and 40 ms and ingoing solids of 34 and 42%. Ingoing sheet temperature=100°C, peak pressure=6.2MPa.

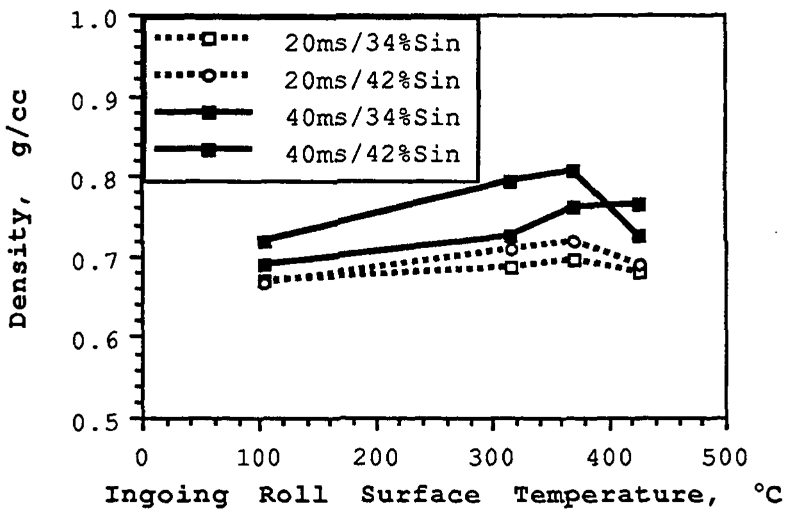

Figure 41: Soft platen density as a function of ingoing roll surface temperature for the pilot-scale impulse drying of 205 gsm linerboard with the prototype ceramic-coated press roll at nip residence times of 20 and 40 ms and ingoing solids of 34 and 42%. Ingoing sheet temperature=100°C, peak pressure=6.2MPa.

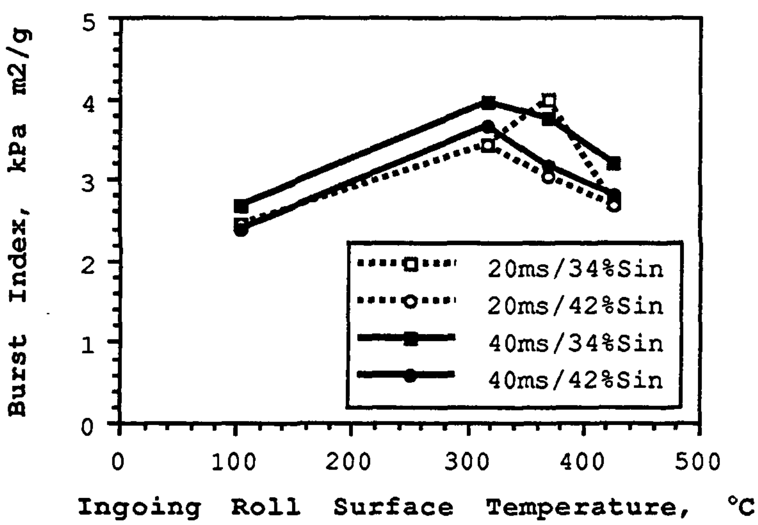

Figure 42: Burst index as a function of ingoing roll surface temperature for the pilot-scale impulse drying of 205 gsm linerboard with the prototype ceramic-coated press roll at nip residence times of 20 and 40 ms and ingoing solids of 34 and 42%. Ingoing sheet temperature=100°C, peak pressure=6.2MPa.

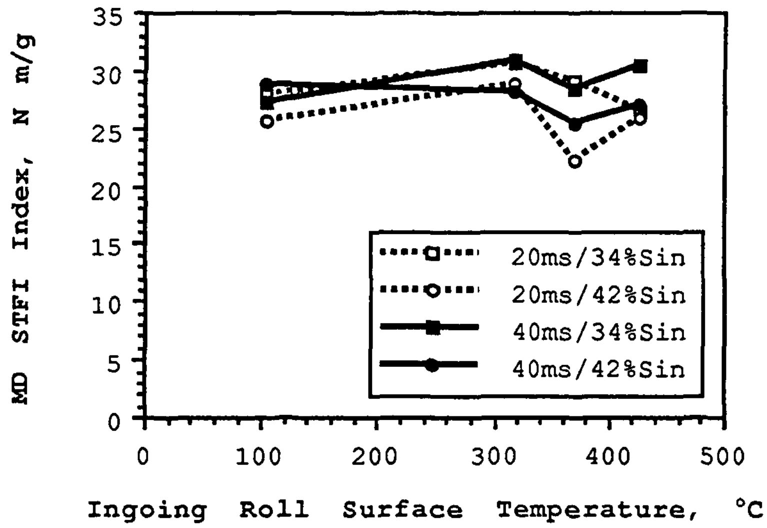

Figure 43: MD STFI compressive index as a function of ingoing roll surface temperature for the pilot-scale impulse drying of 205 gsm linerboard with the prototype ceramic-coated press roll at nip residence times of 20 and 40 ms and ingoing solids of 34 and 42%. Ingoing sheet temperature=100°C, peak pressure=6.2MPa.

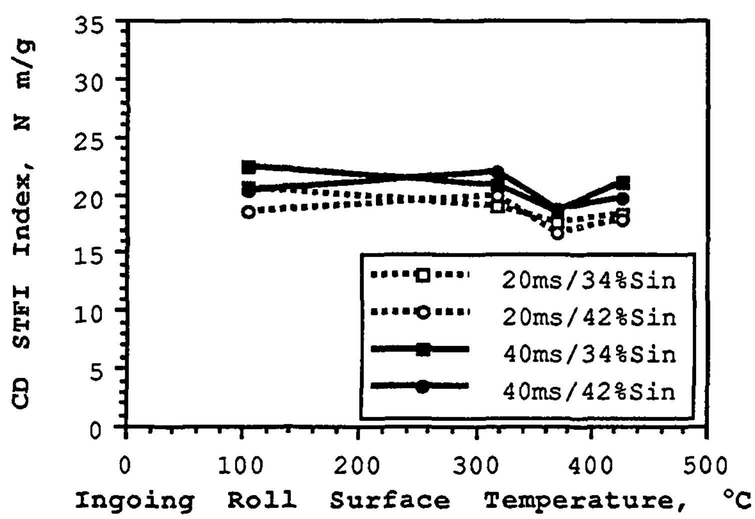

Figure 44: CD STFI compressive index as a function of ingoing roll surface temperature for the pilot-scale impulse drying of 205 gsm linerboard with the prototype ceramic-coated press roll at nip residence times of 20 and 40 ms and ingoing solids of 34 and 42%. Ingoing sheet temperature=100°C, peak pressure=6.2MPa.

Figure 45 shows the relationship between specific elastic modulus and soft platen density for both 20 and 40 ms pilot-scale experiments. Notice that the relationship was independent of ingoing solids and nip residence time. It was also noted that higher modulus at a given soft platen density was observed in the lab-scale experiments conducted with handsheets at an ingoing solids of 30%, see Figure 21.

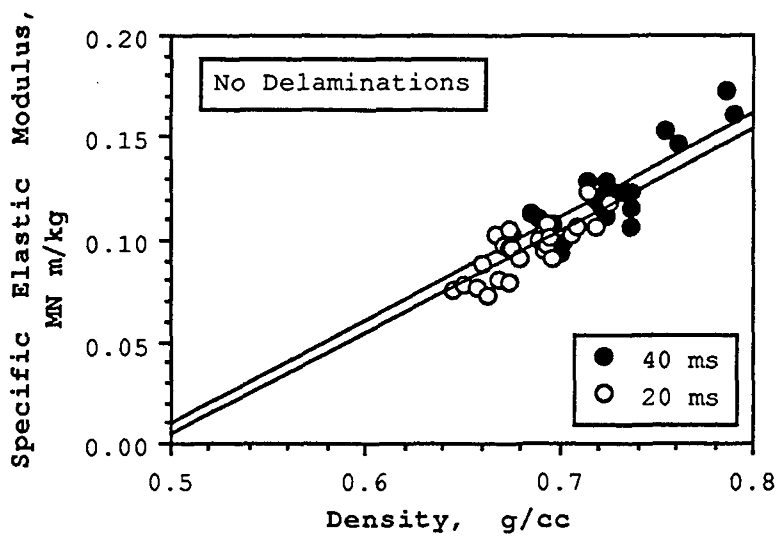

Figure 45: Specific elastic modulus as a function of soft platen density for the pilot-scale impulse drying of 205 gsm linerboard with the prototype ceramic-coated press roll at nip residence times of 20 and 40 ms and ingoing solids of 34 and 42%. Ingoing sheet temperature=100°C, peak pressure=6.2MPa.

COMPARISON OF LAB- AND PILOT-SCALE SIMULATIONS

As heat flux measurements were not attempted on the pilot roll, energy utilization must be deduced from lab-scale simulations. For this purpose, the same web that was impulse dried on the pilot dryer was also impulse dried on the lab-scale simulator.

Figure 46 shows a comparison of outgoing solids, after impulse drying from an ingoing solids of 41% for 40 ms, from pilot- and lab-scale experiments. Lower water removal at low temperatures was consistent with the fact that the lab-scale experiments may have experienced more rewet.

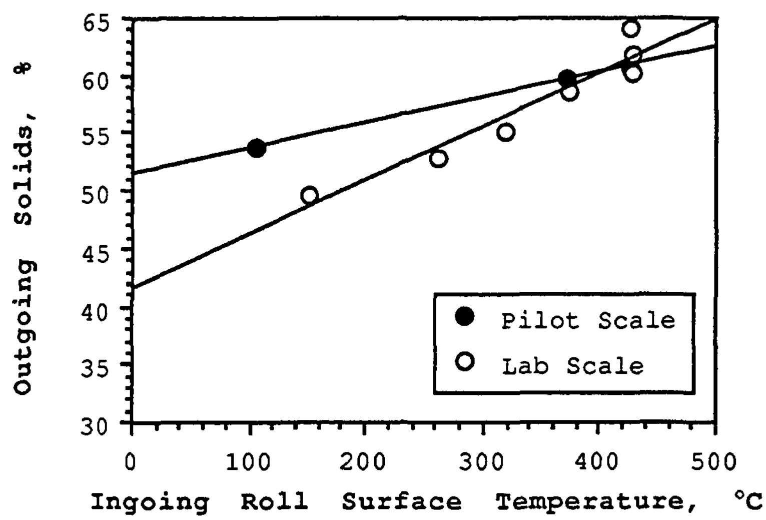

Figure 46: Outgoing solids as a function of initial press surface temperature for pilot- and lab-scale experiments. Dwell time = 40 ms, Ingoing solids = 41%, Peak pressure = 6.2 MPa.

In Figure 47, specific elastic modulus versus initial press surface temperature was compared for the pilot- and lab-scale experiments. The drop-off in modulus at 300°C for the lab-scale experiment is a clear indication of delamination and was verified by scanning electron microscopy. For the same sheets impulse dried on the pilot dryer, delamination was not observed until initial surface temperatures were greater that 371°C. In a repeated pilot experiment at 42% ingoing solids, delamination occurred at surface temperatures in excess of 316°C.

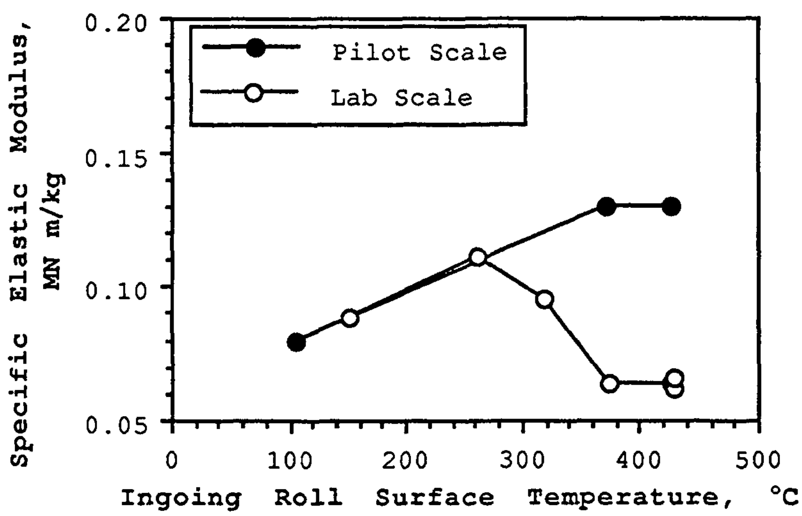

Figure 47: Specific elastic modulus as a function of initial press surface temperature for pilot- and lab-scale experiments. Dwell time = 40 ms, Ingoing solids = 41%, Peak pressure = 6.2 MPa.

Examining the specific elastic modulus-soft platen density relationship in Figure 48, it was observed to be similar to that shown in Figure 45. The agreement of pilot- and lab-scale data suggests that the earlier noted difference in the elastic modulus-soft platen density relationship between lab- and pilot-scale was due to differences in structure between handsheets and sheets formed on the web former.

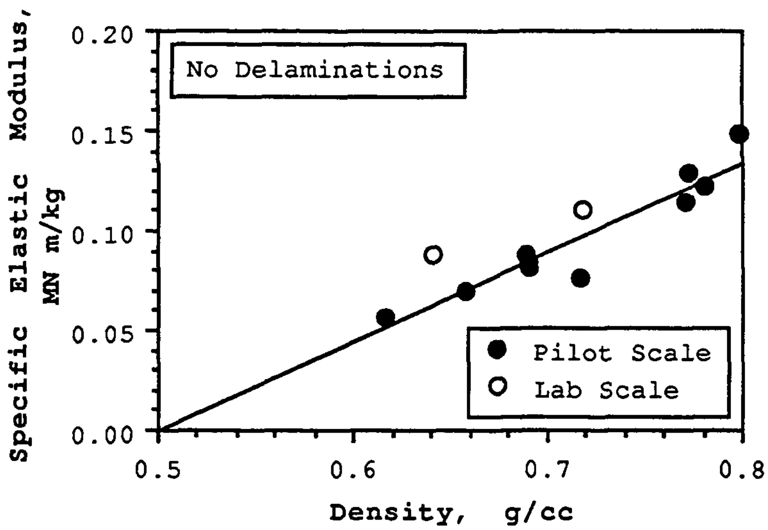

Figure 48: Specific elastic modulus as a function of soft platen density for the pilot-scale and lab-scale impulse drying of 205 gsm linerboard at a dwell time of 40 ms, an ingoing solids of 41% and a peak pressure of 6.2MPa.

Energy transfer from the laboratory-scale simulation is shown in Figure 49. At a temperature corresponding to 371°C, 35 kJ/m^2 was transferred to the sheets. Based on outgoing solids of 60%, incremental energy use of 930 kJ/kg was achieved at these conditions.

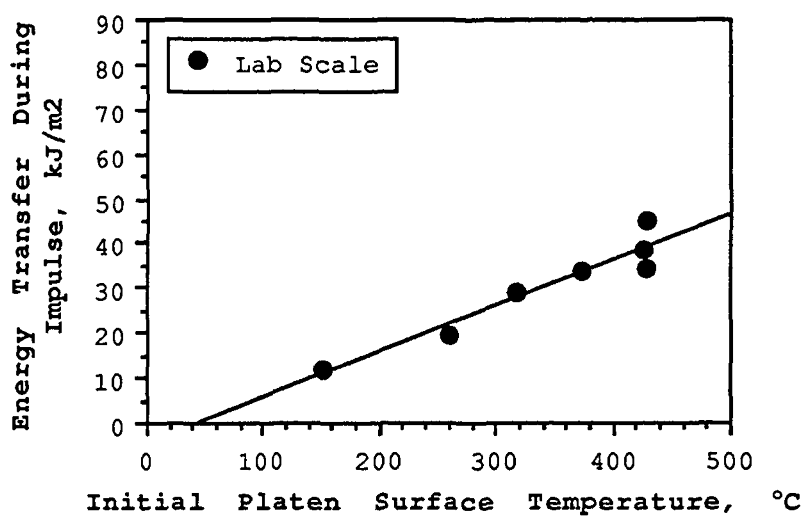

Figure 49: Energy transfer during impulse drying as a function of initial platen surface temperature for impulse drying 205gsm linerboard the prototype ceramic-coated platens with the radiation shield. Dwell time=40ms, ingoing sheet temperature=85°C, ingoing solids=41%.

CONCLUSIONS

The laboratory-scale experiments have demonstrated that the prototype ceramic press roll coating allows operation at high press surface temperatures without sheet delamination. As a consequence, the amount of water removed by impulse drying was substantially more than can be removed by conventional methods. The experiments also show that water removal increases when the surface of the sheet to be impulse dried is kept moist and that sheet physical properties are maximized by operating at high peak pressure.

The pilot-scale impulse drying experiments confirm that substantial improvements over wet pressing can be achieved without inducing sheet delamination. In addition, substantial improvements in sheet properties were also demonstrated. The primary result of the pilot experiments was that the process should be operated at a minimum ingoing dryness of 40% solids at a minimum nip residence time of 40 ms.

IMPULSE DRYING COMMERCIALIZATION PROJECT

Project Objectives

A two-phase program is proposed in which the specialized expertise of IPST, a paper machine vendor and a host paper manufacturer are utilized. In the first phase, occurring in fiscal years 1992 through 1994, design parameters will be decided based on the IPST pilot dryer experiments, and the resulting impulse drying technology will be demonstrated on a pilot paper machine at commercial speeds. In the second phase of the project, occurring in fiscal years 1995 through 1997, the technology will be scaled up and demonstrated on a commercial paper machine.

The objectives of each phase of the project can be summarized in Table 5.

TABLE 5: PROJECT OBJECTIVES

Phase I Objectives	Phase II Objectives
Determine design parameters for pilot paper machine impulse dryer	Scale-up impulse drying system for commercial demonstration.
Fabricate and install impulse dryer on a pilot paper machine	Fabricate and install impulse dryer on commercial paper machine.
Evaluate for a range of grades and furnishes at commercial speed. Document energy utilization and paper property enhancement.	Develop process equipment documentation and control systems and procedures.
Optimize the design of the impulse drying system for maximum energy efficiency and paper properties development.	Demonstrate impulse drying on a continuous basis on the commercial paper machine. Evaluate the durability of components and resulting improvements to energy efficiency and paper properties.

Phase I Project Activities

Impulse drying research at IPST has consisted of process simulations on a laboratory-scale electrohydraulic press and a batch-fed pilot-scale roll press. Additional research and development using these facilities are proposed to resolve a number of design considerations prior to fabrication of the pilot paper machine impulse dryer.

A prototype ceramic coated impulse drying press roll is presently being used to assess the technology for 42-pound linerboard over a range of furnishes and refining levels.The multi-layer low-thermal-mass ceramic coating includes an outer layer of polymer to close the pores of the ceramic coating and to reduce sticking. Laboratory-scale research is in progress to develop a more durable replacement for the polymer layer and to further reduce the thermal mass of the roll coating. It is proposed that the improved ceramic coating be demonstrated on the pilot-scale roll press for a wide range of grades and furnishes to assess the applicability of the technology to these grades. Fabrication of the improved ceramic coating will be subcontracted to companies specializing in plasma spraying. The behavior of these coatings under thermal and mechanical fatigue conditions will also be determined.

Existing pilot-scale data suggest that nip residence times of the order of 40 milliseconds are required to achieve substantial energy efficiency and paper property improvements. Laboratory-scale data further suggest that energy efficiency improves with increased pressure. Pilot roll press experiments are proposed to confirm the need for high pressure and to extend the data base to longer nip residence times to provide a basis for choosing the length of the impulse drying press shoe. In addition, it is proposed that the second nip of the pilot-scale roll press be modified to allow roll heating on either the top or bottom roll. This will allow investigation of multiple short nips as compared to a single long nip. The result of this work will define residence time and pressure requirements.

Existing laboratory- and pilot-scale simulations have been performed using a Haversine pressure curve. As the pilot paper machine impulse dryer will not be limited to a Haversine, it is proposed to upgrade the laboratory-scale simulator so that the shape of the pressure curve can be optimized in combination with the improved ceramic press surface coating.

To facilitate the design of the pilot paper machine impulse drying press roll and roll heating system, it is proposed to use an existing computer model to predict internal roll temperatures and roll re-heating efficiencies.

Based on the results of the above activities, the pilot paper machine impulse dryer module will be designed and fabricated at the equipment vendor and installed on the equipment vendor's pilot paper machine. Ceramic coating of the press roll will be the responsibility of IPST through subcontracts with companies specializing in plasma spray coating.

Ten days worth of trials will be conducted on the pilot paper machine impulse dryer to adjust operating conditions to achieve optimum energy efficiency and paper property development for a grade and furnish contributed by the host mill. Additional furnishes will also be assessed time permitting.

Data from the pilot paper machine impulse drying trials will be used to recommend design changes required to optimize impulse dryer performance.

Phase II Project Activities

Phase II will consist of the design, installation and evaluation of the technology on a commercial paper machine.

The majority of the design work will be carried out by the equipment vendor. However, it is anticipated that laboratory- and pilot-scale experiments may be required to support that design effort.

The equipment vendor will also be responsible for fabrication and installation of the impulse dryer module. Ceramic coating of the press roll will be the responsibility of IPST through subcontracts with companies specializing in plasma spray coating. The equipment vendor, in conjunction with IPST and the host mill, will develop required process equipment documentation and process control systems.

Start-up and adjustments of the commercial impulse dryer will be the responsibility of the equipment vendor, with the assistance and advice of IPST and the host mill.

The commercial demonstration of the impulse dryer will consist of the generation of a conventional drying baseline followed by the impulse drying demonstration. IPST, the vendor and the host mill will be responsible for planning, conducting and documenting the results of the demonstration. Data will include the measurement of energy efficiency and paper properties improvement. The reliability and durability of various components of the impulse dryer will also be assessed.

Equipment Costs and Personnel Requirements

Table 6 through 8 show activity statements for each fiscal year with equipment costs and personnel requirements.

TABLE 6:
EQUIPMENT COSTS AND PERSONNEL REQUIREMENTS
FOR FY 1992 AND 1993

FY 1992	FY 1993
ACTIVITY STATEMENT	**ACTIVITY STATEMENT**
1.Develop and demonstrate a durable low surface energy roll coating and determine energy utilization (Equipment=$11,000)	1.Design and fabricate impulse dryer for pilot paper machine at equipment supplier (Equipment=$1,350,000)
2.Determine on IPST pilot the range of grades and furnishes for which ceramic press roll technology is applicable	2. Conduct laboratory and pilot-scale experiments to support design effort
3.Thermal and mechanical fatigue tests on most promising ceramic press roll coating	
4.Extend IPST pilot data to lower pressures and longer dwell times	
5.Modify IPST pilot to allow two nip drying on same side of paper and compare one 40 ms nip to two 20 ms nips (Equipment=$100,000)	
6.Modify lab-scale simulator to allow programmable pressure profiles and determine best profile (Equipment=$62,000)	
7.Perform calculations to design roll heating system for commercial speeds	

PERSONNEL REQUIREMENT	PERSONNEL REQUIREMENT
IPST: Pr.Engr(1), Tech (4) CO-OP (1)	IPST: Pr.Engr(1), Tech (4) CO-OP (1)
VENDOR:Sen Engr(1/2)	VENDOR:Sen Engr(1), Design(2) Tech(1)
	HOST MILL:Sen Engr(1)

TABLE 7:
EQUIPMENT COSTS AND PERSONNEL REQUIREMENTS
FOR FY 1994 AND 1995

FY 1994	FY 1995
ACTIVITY STATEMENT	**ACTIVITY STATEMENT**
1.Installation of impulse dryer on Vendor's pilot paper machine (Installation=$1,350,000)	1.Design impulse dryer for commercial demonstration at Host Mill
2.Evaluate for range of furnishes at commercial speed. Documenting water removal, property development and energy utilization. (est 10 days) (Pilot Machine Time +Furnish)=$200,000	2.Conduct laboratory- and pilot-scale experiment as needed to support design effort
3.Optimize design of impulse drying system	

PERSONNEL REQUIREMENT	PERSONNEL REQUIREMENT
IPST: Pr.Engr(1), Tech (4) CO-OP (1)	IPST: Pr.Engr(1), Tech (4) CO-OP (1)
VENDOR:Sen Engr(1), Design(1), Tech(2)	VENDOR:Sen Engr(1), Engr(1) Design(2)
HOST MILL:Sen Engr(1)	HOST MILL:Sen.Engr(1), Engr(1)

TABLE 8:
EQUIPMENT COSTS AND PERSONNEL REQUIREMENTS
FOR FY 1996 AND 1997

FY 1996	FY 1997
ACTIVITY STATEMENT	**ACTIVITY STATEMENT**
1.Fabricate and install impulse dryer on commercial paper machine (Hardware & Installation=$8-25 million	1.Commercial demonstration of impulse drying on a continuous basis
2.Develop process equipment documentation and control systems	2.Evaluate system component durability and performance
3.Start-up of impulse dryer on commercial paper machine	3.Document water removal, property development and energy efficiency improvement
4.Conduct preliminary trials	

PERSONNEL REQUIREMENT	PERSONNEL REQUIREMENT
IPST: Pr.Engr(1), Tech (4), CO-OP (1)	IPST: Pr.Engr(1), Tech (2)
VENDOR:Sen Engr(1),Engr(1), Tech(3)	VENDOR:Sen Engr(1)
HOST MILL:Sen Engr(1), Engr(1), Tech(4)	HOST MILL:Sen Engr(1), Engr(1), Tech(4)

REFERENCES

1. Sprague, C.,Lavery, H.P., High-Intensity Drying Processes-Impulse Drying, Report 1 for Department of Energy Contract FGO2-85CE40738, DOE/CE/40738-T1, August, 1985.

2. Lavery, H.P., High-Intensity Drying Processes-Impulse Drying, Report 2 for Department of Energy Contract FGO2-85CE40738, DOE/CE/40738-T2, February, 1987.

3. Lavery, H.P., High-Intensity Drying Processes-Impulse Drying, Report 3 for Department of Energy Contract FGO2-85CE40738, DOE/CE/40738-T3, February, 1988.

4. Arenander, S. and Wahren, D., Impulse Drying Adds New Dimension to Water Removal, TAPPI Journal, Vol.66, No. 9, September 1983.

5. Burton, S., A Dynamic Simulation of Impulse Drying, A190 Project, The Institute of Paper Chemistry, May 1983.

6. Burton, S., Ph.D. Thesis,"An Investigation of Z-direction Density Profile Development During Impulse Drying", The Institute of Paper Chemistry, June 1986.

7. Crouse, J.W.; Woo, Y.D.; and Sprague, C.H., Delamination: A Stumbling Block To Implementation Of Impulse Drying Technology For Linerboard, Tappi Engineering Conference, Atlanta, Georgia, September 13, 1989.

8. Orloff, D.I., High-Intensity Drying Processes-Impulse Drying, Report 4 for Department of Energy Contract FGO2-85CE40738, DOE/CE/40738-T4, May 1989.

9. Santkuyl, R., Effect of Surface Material on Delamination in Impulse Drying, A190 Project, The Institute of Paper Chemistry, 1989.

10. Orloff, D.I., et al., Method and Apparatus for Drying Web, U.S. Patent Application Number 417,261, Filed October 5, 1989.

11. Orloff, D.I., Impulse Drying: Fundamentals of Delamination and Its Control, Presented at the 1989 National AIChE Meeting, September 1989.

12. Orloff, D.I., High-Intensity Drying Processes-Impulse Drying, Report 5 for Department of Energy Contract FGO2-85CE40738, DOE/CE/40738-T5, September 1990.

13. Habeger, C.C. and Wink, W.A., Ultrasonic Velocity Measurements in the Thickness Direction of Paper, Journal of Applied Polymer Science, Vol. 32, 4503-4540 (1986).

14. Orloff, D.I., Impulse Drying Of Linerboard: Control Of Delamination, Proceedings of the 77th Annual Meeting of the Technical Section of the Canadian Pulp and Paper Association, Montreal, Quebec, January 1991.

15. Orloff, D.I., Impulse Drying: Heterogeneous Press Surfaces Offer New Product Opportunities, Proceedings 1991 Nonwovens Conference, TAPPI Press, May 1991.

APPENDIX

SINGLE FELTED PRESSING BASELINE

For proper evaluation, impulse drying should be compared to single felted extended nip wet pressing. Such a comparison should show the improvement in water removal and sheet physical properties contributed by the impulse drying mechanism. To provide this comparison, a single felted wet pressing baseline study was carried out. A steel platen coated with polymer release agent was used. Handsheets at various ingoing solids were preheated by steaming and then wet pressed with the heated steel platen. The platen was heated to the temperature of the preheated sheet.

Figures A1, A2 and A3 show the moisture ratio change resulting from pressing sheets preheated to three temperatures at three different peak pressures, all at a dwell time of 20 ms.

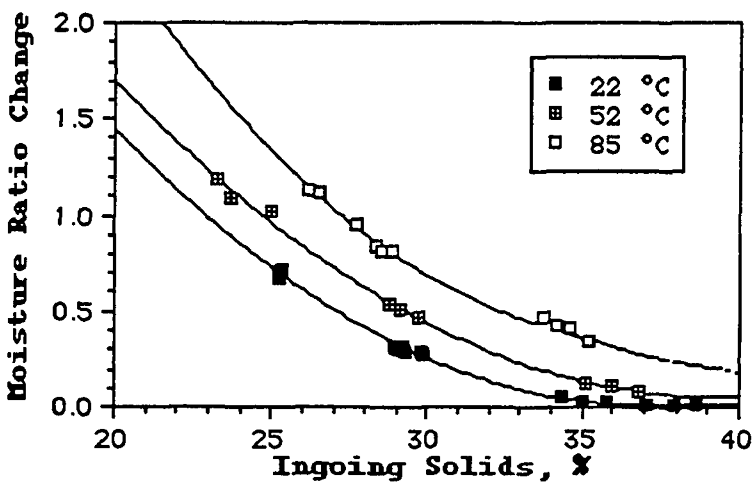

Figure A1: Moisture ratio change for single felted wet pressing of 205 gsm linerboard as a function of ingoing solids and ingoing sheet temperature. Dwell time=20ms, peak pressure=1.7MPa, impulse=0.015MPas.

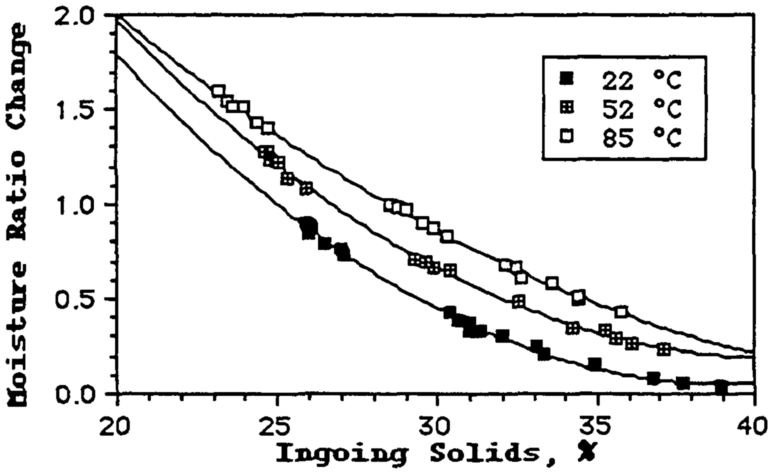

Figure A2: Moisture ratio change for single felted wet pressing of 205 gsm linerboard as a function of ingoing solids and ingoing sheet temperature. Dwell time=20ms, peak pressure=3.1MPa, impulse=0.028MPas.

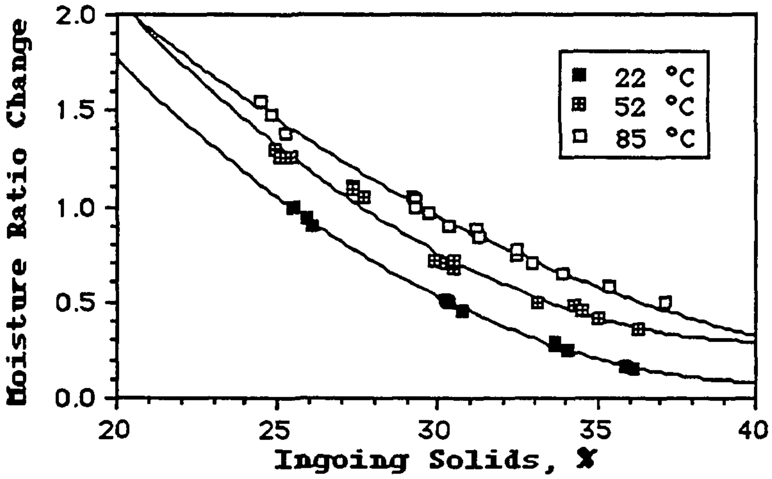

Figure A3: Moisture ratio change for single felted wet pressing of 205 gsm linerboard as a function of ingoing solids and ingoing sheet temperature. Dwell time=20ms, peak pressure=4.8MPa, impulse=0.044MPas.

As expected, water removal increased with increasing ingoing sheet temperature and with increasing peak pressure. Pressing has a diminishing effect as the ingoing solids increased.

Figure A4 shows similar data obtained at a dwell time of 60 ms and a peak pressure of 3.13 MPa.

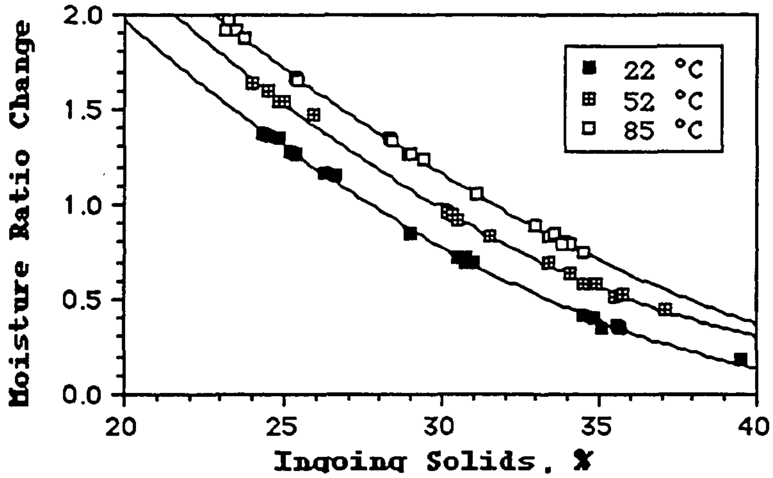

Figure A4: Moisture ratio change for single felted wet pressing of 205 gsm linerboard as a function of ingoing solids and ingoing sheet temperature. Dwell time=60ms, peak pressure=3.1MPa, impulse=0.140MPas.

Using the data shown in Figures A1 through A4, water removal could be predicted from impulse, independent of peak pressure. Figure A5 shows this result for sheets having an ingoing solids of 30%. It was concluded that the furnish was flow controlled.

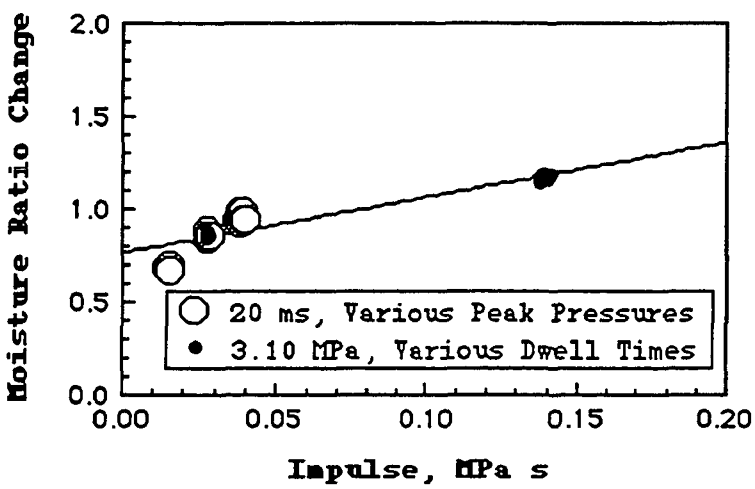

Figure A5: Moisture ratio change for single felted wet pressing of 205 gsm linerboard as a function of impulse. Ingoing sheet temperature=85°C, ingoing solids=30%.

Water removal was correlated to ingoing sheet temperature and impulse, as shown in Figure A6. The improvement in water removal with increased ingoing sheet temperature may be attributed to a reduction in the viscosity of water and increased sheet compressibility. While the present data are at lower impulse than those of Back (18), they are consistent with his data.

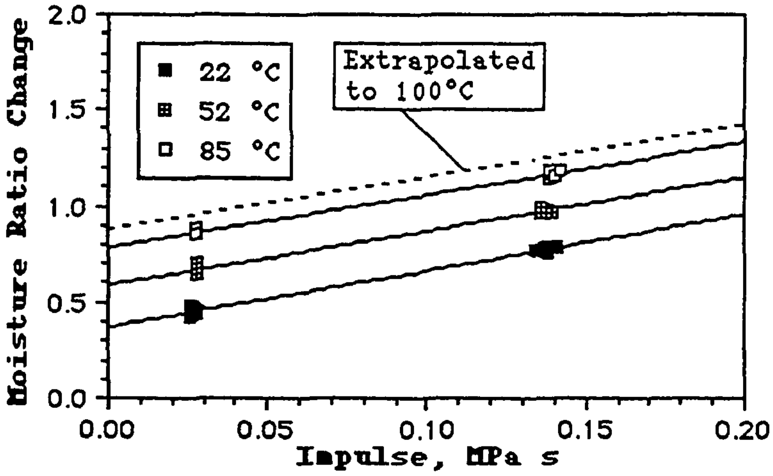

Figure A6: Moisture ratio change for single felted wet pressing of 205 gsm linerboard as a function of impulse and ingoing sheet temperature. Ingoing solids=30%.

ACKNOWLEDGMENTS

The work reported in this paper was supported by the members of the Institute of Paper Science and Technology and by the U.S. Department of Energy Office of Industrial Programs through Grant No. DE-FG02-85CE40738. Their support is gratefully acknowledged. In addition, the fine efforts of all the members of the impulse drying project team at the Institute are acknowledged. P. Phelan conducted laboratory-scale experiments while M. Schaepe conducted the pilot-scale experiments. Excellent experimental help was also provided by D. Brennen, A. Granberg of STFI, and Georgia Tech co-op students J. Norman and R. Shelley.

The author would also like to recognize the valued assistance of W. Lenling of Fisher- Barton Corporation and Sandia National Laboratory for fabricating the prototype platen and coating the pilot press roll. The author is also grateful to Professor R. Ellis and Professor J. Lindsay for their many helpful suggestions and for Professor Lindsay's assistance in measuring sheet permeability.